

International Doctorate Program in
Molecular Oncology and
Endocrinology
Doctorate School in Molecular
Medicine

XIX cycle - 2003–2007
Coordinator: Prof. Giancarlo Vecchio

**“H4(D10S170), a gene frequently
rearranged with RET in papillary
thyroid carcinomas: functional
characterization.”**

Vincenza Leone

University of Naples Federico II
Dipartimento di Biologia e Patologia Cellulare e
Molecolare
“L. Califano”

Administrative Location

Dipartimento di Biologia e Patologia Cellulare e Molecolare “L. Califano”
Università degli Studi di Napoli Federico II

Partner Institutions

Italian Institutions

Università degli Studi di Napoli “Federico II”, Naples, Italy
Istituto di Endocrinologia ed Oncologia Sperimentale “G. Salvatore”, CNR, Naples, Italy
Seconda Università di Napoli, Naples, Italy
Università del Sannio, Benevento, Italy
Università di Genova, Genoa, Italy
Università di Padova, Padua, Italy

Foreign Institutions

Johns Hopkins School of Medicine, Baltimore, MD, USA
Johns Hopkins Krieger School of Arts and Sciences, Baltimore, MD, USA
National Institutes of Health, Bethesda, MD, USA
Ohio State University, Columbus, OH, USA
Université Paris Sud XI, Paris, France
Universidad Autonoma de Madrid, Spain
Centro de Investigaciones Oncologicas (CNIO), Spain
Universidade Federal de Sao Paulo, Brazil
Albert Einstein College of Medicine of Yeshiwa University, USA

Supporting Institutions

Università degli Studi di Napoli “Federico II”, Naples, Italy
Ministero dell’Università e della Ricerca
Istituto Superiore di Oncologia (ISO)
Terry Fox Foundation, Canada
Istituto di Endocrinologia ed Oncologia Sperimentale “G. Salvatore”, CNR, Naples, Italy
Centro Regionale di Competenza in Genomica (GEAR)
Università Italo-Francese

Faculty

Italian Faculty

Giancarlo Vecchio, MD, Co-ordinator
Francesco Beguinot, MD
Angelo Raffaele Bianco, MD
Francesca Carlomagno, MD
Gabriella Castoria, MD
Angela Celetti, MD
Vincenzo Ciminale, MD
Annamaria Cirafici, PhD
Annamaria Colao, MD
Alma Contegiacomo, MD
Sabino De Placido, MD
Monica Fedele, PhD
Pietro Formisano, MD
Alfredo Fusco, MD
Massimo Imbriaco, MD
Paolo Laccetti, MD
Antonio Leonardi, MD
Barbara Majello, PhD
Rosa Marina Melillo, MD
Claudia Miele, PhD
Francesco Oriente, MD
Roberto Pacelli, MD
Giuseppe Palumbo, PhD
Silvio Parodi, MD
Giuseppe Portella, MD
Giorgio Punzo, MD
Antonio Rosato, MD
Massimo Santoro, MD
Giampaolo Tortora, MD
Donatella Tramontano, PhD
Giancarlo Troncone, MD
Bianca Maria Veneziani, MD

Foreign Faculty

National Institutes of Health (USA)

Michael M. Gottesman, MD
Silvio Gutkind, PhD
Stephen Marx, MD
Ira Pastan, MD
Phill Gorden, MD

Johns Hopkins School of Medicine (USA)

Vincenzo Casolaro, MD
Pierre Coulombe, PhD
James G. Herman MD
Robert Schleimer, PhD

Johns Hopkins Krieger School of Arts and Sciences (USA)

Eaton E. Lattman, MD

Ohio State University, Columbus (USA)

Carlo M. Croce, MD

Albert Einstein College of Medicine of Yeshiva University (USA)

Luciano D'Adamio, MD
Nancy Carrasco, MD

Université Paris Sud XI (France)

Martin Schlumberger, MD
Jean Michel Bidart, MD

Universidad Autonoma de Madrid (Spain)

Juan Bernal, MD, PhD
Pilar Santisteban

Centro de Investigaciones Oncologicas (Spain)

Mariano Barbacid, MD

Universidade Federal de Sao Paulo (Brazil)

Janete Maria Cerutti
Rui Maciel

“H4(D10S170), a gene frequently rearranged with RET in papillary thyroid carcinomas: functional characterization.”

TABLE OF CONTENTS

LIST OF PUBLICATIONS.....	7
ABSTRACT.....	8
1. BACKGROUND.....	9
1.1 The thyroid gland.....	9
1.2 Thyroid follicular cell carcinomas.....	10
1.3 Papillary thyroid carcinoma (PTC).....	13
1.4 Transcription factor cAMP response element-binding protein CREB ...	19
1.5 H4.....	21
2. AIMS OF THE STUDY.....	23
3. MATERIALS AND METHOD.....	25
3.1 Cell cultures and treatments and trasfection.	25
3.2 Expression constructs.....	25
3.3 Transactivation assay	25
3.4 In vitro proteins translation and pull down assay.....	25
3.5 Total protein extracts Western blotting, and immunoprecipitation assay.....	26
3.6 Nuclear extracts preparation.....	27
3.7 Electrophoretic mobility shift assay (EMSA) and supershift assay.....	27
3.8 RNA isolation	28
3.9 Reverse transcriptase and Real Time PCR analysis.....	28
3.10 HDAC activity.	29
3.11 Chromatin immunoprecipitation (ChIp) and Re-ChIp assays.....	29
3.12 Mouse H4 Gene Targeting and Mating.....	30
3.13 Growth Rate	31
3.14 Apoptosis detection.....	31
3.15 Cell cycle analysis.....	31
3.16 MEFs culture.....	31
4. RESULTS AND DISCUSSION.....	33
4.1 H4 binds CREB1.....	33
4.2 H4 inhibits the transcriptional activity of CREB1.....	35
4.3 H4 reduces CREB1 target genes trascription	36
4.4 H4 reduces CREB1 binding to CRE element.....	37
4.5 H4 requires Hdac activity to repress CREB1 target genes transcription...	38
4.6 H4 associates with HDAC1.....	42
4.7 H4 interacts in vivo with the AREG promoter and recruits HDAC1 and reduces the binding of CREB1.....	43
4.8 H4 expression is correlated with AREG promoter deacetylation.....	45
4.9 Knock-out H4 mice.....	46
4.10 H4 KO affects cell proliferation.....	47
4.11 Cell cycle distribution.....	48
4.12 Cyclin and CDK Expression pattern is altered in H4 -/- MEFs.....	48
4.13 H4 -/- MEFs induce apoptosis.....	50

4.14 Activation of CREB1 in H4 -/- MEFs.....	50
5. CONCLUSIONS.....	52
6. ACKNOWLEDGEMENTS.....	54
7. REFERENCES.....	55

LIST OF PUBLICATIONS

- 1) di Palma A, Matarese G, **Leone V**, Di Matola T, Acquaviva F, Acquaviva AM, Ricchi P.
Aspirin reduces the outcome of anticancer therapy in Meth A-bearing mice through activation of AKT-glycogen synthase kinase signaling.
Mol Cancer Ther. 2006 May;5(5):1318-24.

- 2) Berlingieri MT, Pallante P, Guida M, Nappi C, Masciullo V, Scambia G, Ferraro A, **Leone V**, Sboner A, Barbareschi M, Ferro A, Troncone G, Fusco A.
UbcH10 expression may be a useful tool in the prognosis of ovarian carcinomas.
Oncogene. 2007 Mar 29;26(14):2136-40. Epub 2006 Oct 2.

- 3) Visone R, Pallante P, Vecchione A, Cirombella R, Ferracin M, Ferraro A, Volinia S, Coluzzi S, **Leone V**, Borbone E, Liu CG, Petrocca F, Troncone G, Calin GA, Scarpa A, Colato C, Tallini G, Santoro M, Croce CM, Fusco A.
Specific microRNAs are downregulated in human thyroid anaplastic carcinomas.
Oncogene. 2007 Jun 11;

- 4) **Leone V**, di Palma A, Ricchi P, Acquaviva F, Giannouli M, Di Prisco AM, Iuliano F, Acquaviva AM.
PGE2 inhibits apoptosis in human adenocarcinoma Caco-2 cell line through RAS-PI3-kinase association and cAMP dependent Kinase A activation.
Am J Physiol Gastrointest Liver Physiol. 2007 Jul 19;

- 5) Visone R, Russo L, Pallante P, De martino I, Ferraro A, **Leone V**, Borbone E, Petrocca F, Alder H, Croce CM, Fusco A.
miR-221 and miR-222, both overexpressed in human thyroid papillare carcinomas, regulate
p27^{kip1} protein levels and cell cycle.
Endocrine Related Cancer- 2007 Sept 14.

Abstract

Papillary thyroid carcinoma (PTC) is the most common thyroid malignancy and the biological behaviour of PTC varies widely from indolent microcarcinomas, growing slowly with little or no invasion, to invasive tumours that metastasize and can cause death.

Most human thyroid papillary carcinomas are characterized by rearrangements of the RET protooncogene with a number of heterologous genes, which generate the RET/papillary thyroid carcinoma (PTC) oncogenes.

In the various RET/PTC oncoproteins, little is known about the normal role of the 5' fusion partners. Some common features such as constitutive expression and the presence of dimerization domains have been observed for all the RET-fused genes. The ubiquitously expressed promoters of the 5'-fused sequences are responsible for the ectopic expression of RET in epithelial thyroid follicular cells, which do not normally express this protooncogene. Although this indicates that disruption of the normal regulation of the RET kinase is critical to the transforming properties, less is known about whether disruption of the normal function of the 5' partner gene might also have an important role. To address this point, the identification of the normal physiological function of the heterologous RET fusion partners is required. Therefore, we have characterized the product of the first and most frequently observed RET-fused gene, H4(D10S170).

We conducted a study for functional characterization of H4 gene. Our results demonstrated that H4 is responsible for the transcriptional repression of CREB1 target genes by a chromatin-dependent mechanism. We demonstrated in this study that H4 requires histone deacetylase (HDAC) activity to repress the transcription and the treatment with trichostatin A (TSA), an HDAC inhibitor, is useful to block the repressor effect of H4. Moreover, H4 associates with histone deacetylase 1 (HDAC1) and recruits HDAC1 on CRE site of CREB1 target genes, in particular AREG (amphiregulin) promoter gene.

The H4-mediated recruitment of HDAC1 increased deacetylation of histones H3 and contributes to close chromatin structure and to repress promoter activity.

1. BACKGROUND

1.1 The thyroid gland

The thyroid gland is the largest endocrine organ in humans (Kondo 2006). It is located in the neck region, on the anterior surface of the trachea, and is formed by two distinct cell types, the follicular cells (TFC) and the parafollicular or C cells (De Felice and Di Lauro 2004). The TFC constitute the most numerous cell population and form the thyroid follicles, spherical structures that store and release the thyroid hormones (Mauchamp et al. 1998). The C cells are located between follicles, mostly in a parafollicular position (Figure 1).

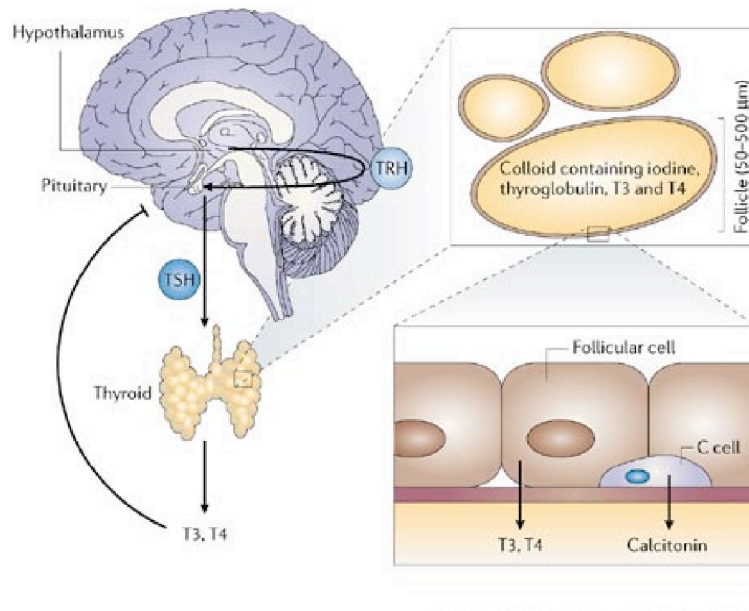


Figure 1 The thyroid gland and the hypothalamic–pituitary axis

In the figure is shown the hypothalamic–pituitary axis with negative feedback by the thyroid hormones and the general architecture of the thyroid gland with the parafollicular cells interspersed in small groups among the follicles in the intermediate part of the thyroid lobes.

These two cell types take origine from two different embryological structures: the thyroid anlage for the TFC and the ultimobranchial bodies for the C cells. The thyroid anlage is an area enclosing a small group of endodermal cells, and it is located on the midline of the embryonic mouth cavity in its posterior part. The ultimobranchial bodies are a pair of transient embryonic structures derived from the fourth pharyngeal pouch and located symmetrically on the sides of the developing neck: C cell precursors migrate from the neural crest (Le Douarin et al. 1974) in these structures (Fontaine J 1979). The cells of the thyroid anlage and the ultimobranchial bodies migrate from their respective sites of origin and ultimately merge in the definitive thyroid gland. Once merged, the thyroid anlage and the ultimobranchial bodies disappear and their cells disperse in the adult thyroid gland. At this point the cells from the anlage continue to organize the thyroid follicles, whereas the C cells scatter within the interfollicular space. Interestingly, in some animals, the ultimobranchial structures remain distinct from the rest of the thyroid gland (Gorbman A 1986). In the adult human, the gland has a butterfly shape and has a weight 15–25 g. It is comprised of aggregates (lobules) of spherical follicles that are filled with colloid. The follicles range in size from 50–500 μm and are lined by cuboidal-to-flat follicular epithelial cells. The main functions of the thyroid gland are synthesis, storage and secretion of thyroid hormones, L-triiodothyronine (T3) and L-thyroxine (T4) (Kondo et al. 2006). This mechanism is under the control of the hypothalamic-pituitary axis with negative feedback by the thyroid hormones: thyrotropin releasing hormone (TRH), secreted from the hypothalamus, stimulates the release of thyroid-stimulating hormone (TSH) from the anterior pituitary gland. TSH, then, stimulates the follicular cells to synthesize and secrete thyroid hormones. Disruption of thyroid hormone homeostasis results in hypothyroidism, goiter and in childhood cretinism (Kondo et al. 2006).

The parafollicular C-cells secrete calcitonin, which is important for the bone formation. Its secretion is stimulated by elevate calcium concentration in the serum (Lin et al. 1991; Nicholson et al. 1986).

1.2 Thyroid follicular cell carcinomas

Malignant tumors of the thyroid gland comprise a heterogeneous group of neoplasms with distinctive clinical and pathological characteristics. Approximately 90% of these tumors are derived from follicular cells while the remainders originate from the calcitonin-producing C-cells or from other cell types.

Follicular-cell-derived carcinomas are broadly divided into well-differentiated, poorly differentiated and undifferentiated types on the basis of histological and clinical parameters (Table 1). Well-differentiated thyroid carcinoma includes papillary and follicular types. Although initially defined by architectural criteria, the histological diagnosis of papillary carcinoma rests on a number of nuclear features that predict the propensity for metastasis to local lymph nodes. The diagnosis of this most frequent type of thyroid malignancy (85–90% of

thyroid malignancies) has been increasing, possibly owing to the changing recognition of nuclear morphological criteria. On the other hand, follicular thyroid carcinoma is characterized by haematogenous spread, and the frequency of its diagnosis has been decreasing (LiVolsi 1994). Most well-differentiated thyroid cancers behave in an indolent manner and have an excellent prognosis.

By contrast, undifferentiated or anaplastic thyroid carcinoma is a highly aggressive and lethal tumour (World Health Organization Classification of Tumors, Kebebew 2005). The presentation is dramatic, with a rapidly enlarging neck mass that invades adjacent tissues. There is currently no effective treatment and death usually occurs within 1 year of diagnosis. Poorly differentiated thyroid carcinomas are morphologically and behaviourally intermediate between well-differentiated and undifferentiated thyroid carcinomas (Carcangiu 1984, Rodriguez 1998) (Table 1) and pursue an aggressive course with mean 5 year survivals in the range of 50%. Medullary carcinomas, which originate from the intrathyroidal C-cells, comprise approximately 10% of primary thyroid tumors and have 5 and 10-years survivals of approximately 80% and 70%, respectively.

Tumour type	Prevalence	Sex ratio (female: male)	Age (years)	Lymph-node metastasis	Distant metastasis	Survival rate (5 year)
Papillary thyroid carcinoma	85–90%	2:1–4:1	20–50	<50%	5–7%	>90%
Follicular thyroid carcinoma	<10%	2:1–3:1	40–60	<5%	20%	>90%
Poorly differentiated thyroid carcinoma	rare–7%	0.4:1–2.1:1	50–60	30–80%	30–80%	50%
Undifferentiated thyroid carcinoma	2%	15:1	60–80	40%	20–50%	1–17%
Medullary thyroid carcinoma	3%	1:1–1.2:1	30–60	50%	15%	80%
Mixed medullary and follicular-cell carcinoma	rare					

Table 1 | Clinico-pathological features of thyroid cancer

The theory of sequential progression of well-differentiated thyroid carcinoma through the spectrum of poorly differentiated to undifferentiated thyroid carcinoma (Figure 2) is supported by the presence of pre- or co-existing well-differentiated thyroid carcinoma with less differentiated types, and the common core of genetic loci with identical allelic imbalances in co-existing well-differentiated components (Van der Laan 1993, Hunt 2003).

Risk factors, such as exposure to radiation, induce genomic instability through direct and indirect mechanisms, resulting in early genetic alterations that involve the mitogen-activated protein kinase (MAPK) signalling pathway. Oncogenic activation of MAPK signalling further increases genomic instability, leading to later genetic alterations that involve other signalling pathways, cell-cycle regulators and various adhesion molecules. Accelerating the interactions between genomic instability and genetic alterations promotes progression from well-differentiated to undifferentiated thyroid carcinoma. On the basis of clinical, histological and molecular observations, three distinct pathways are proposed for neoplastic proliferation of thyroid follicular cells, including hyper-functioning follicular thyroid adenoma (tumours that are almost always benign lesions without a propensity for progression), follicular thyroid carcinoma and papillary thyroid carcinoma. In papillary thyroid carcinoma (PTC), genetic events involve RET and TRK (rearrangements) (Pierotti and Greco 2006) and BRAF(Xing 2005) and RAS (Suarez et al. 1990) (mutations), although RAS mutations are uncommon except in the follicular variant of PTC. These genetic alterations, which rarely overlap in the same tumor, result in signalling abnormalities in the mitogen activated protein kinase pathway. In contrast, genetic alterations in follicular carcinomas include PAX8-PPAR γ translocations (Kroll et al. 2000) and RAS mutations, while mutations of PI3KCA and p53 have been implicated in the development and progression of poorly differentiated and undifferentiated (anaplastic) thyroid carcinomas (Donghi et al. 1993, Fagin et al. 1993). Germline mutations of RET are responsible for the development of heritable forms of medullary thyroid carcinoma (MTC) while somatic mutations of this gene are found in a significant proportion of sporadic MTCs (Figure 2).

Multi-step tumorigenesis in thyroid carcinomas of follicular origin

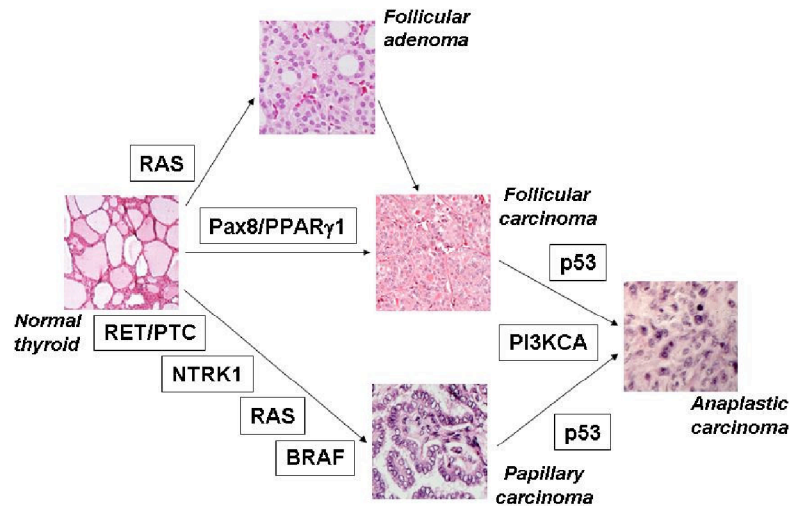


Figure 2 Model of multi-step carcinogenesis of thyroid neoplasms.

On the basis of clinical, histological and molecular observations, three distinct pathways are proposed for neoplastic proliferation of thyroid follicular cells, including hyper-functioning follicular thyroid adenoma (tumours that are almost always benign lesions without a propensity for progression), follicular thyroid carcinoma and papillary thyroid carcinoma. Genetic defects that result in activation of RET or BRAF represent early, frequent initiating events that can be associated with radiation exposure. Most poorly differentiated and undifferentiated thyroid carcinomas are considered to derive from pre-existing well-differentiated thyroid carcinoma through additional genetic events, including p53 inactivation, but de novo occurrence might also occur.

1.3 Papillary thyroid carcinoma (PTC)

Papillary thyroid carcinoma (PTC) is currently defined as a malignant epithelial tumor that shows evidence of follicular cell differentiation and that is characterized by a set of distinctive nuclear features (LiVolsi 2004). In most series, these tumors comprise approximately 90% of all thyroid cancers. Although thyroid tumors are uncommon in childhood, PTCs represent the most common pediatric thyroid malignancy.

Incidence:

Most PTCs in adults occur in patients between 20 and 50 years of age with a female to male ratio of 4–5:1. The incidence of thyroid cancer has increased from 3.6 to 8.7 per 100,000 between 1973 and 2000 primarily due to the increased detection of small (subclinical) papillary carcinomas (Davies 2006).

The diagnostic features of PTC:

The diagnostic features of PTC include nuclear enlargement and irregularity, overlapping, clearing (ground glass or Orphan Annie appearance), grooves, and pseudoinclusions (LiVolsi 2004). Conventional PTCs are characterized by a complex branching architecture in which the surfaces of the papillary cores are covered by neoplastic cells. Varying degrees of squamous metaplasia are common and many tumours also contain follicular structures with nuclear features that are identical to those present in the papillary components. Psammoma bodies are present in approximately 50% of cases and occur typically within the stroma or lymphatic channels. Intratumoural fibrosis and lymphocytic infiltrates are also common features of these tumours.

Variants of PTC:

Numerous variants of PTC are recognized (De Lellis 2006). One of the most common and most diagnostically challenging is the follicular variant. These tumors may be encapsulated or non-encapsulated and are composed almost exclusively of follicles having the characteristic nuclear features of PTC. Inter-observation variation in the diagnosis of these tumors, particularly the encapsulated type, is high since the nuclear features may be focal or poorly developed (Lloyd 2004). Lymph node metastases are less common in the follicular variant than in conventional PTCs. Microfollicular, oncocytic, Warthin-like, and clear cell variants have a prognosis that is similar to conventional PTCs (Table II).

The solid variant comprises approximately 8% of sporadic PTCs and is relatively common in children following radiation exposure. This variant is associated with a slightly higher frequency of distant metastases and a somewhat less favorable prognosis than conventional PTC (Nikiforov Y 2002, Nikiforov YE 2001). The diffuse sclerosing variant is more common in children than adults with a higher frequency of pulmonary metastases than conventional PTCs although overall survivals do not differ significantly. Both tall cell and columnar cell variants are thought to have a worse prognosis than conventional PTCs; however, stage and grade may be more important than histological subtypes (Asklen 2000). The prognosis of PTCs with poorly differentiated, undifferentiated, or squamous carcinoma components depends on the proportion of the non-PTC component.

The term papillary “microcarcinoma” is reserved for those tumors measuring less than 1 cm in diameter. Although most of these tumors have follicular or papillary architectural features, any of the variants may measure less than 1 cm. Papillary microcarcinomas are extremely common, occurring in up to 30%

of autopsies and in up to 24% of surgical thyroidectomies performed for disorders unrelated to PTC (Fink1996

TABLE II. Papillary Thyroid Carcinoma (PTC) Variants

Follicular
Macrofollicular
Oncocytic
Warthin-like
Clear cell
Diffuse sclerosing
PTC with fasciitis-like stroma
Solid
Tall cell
Columnar cell
PTC with minor poorly differentiated component
PTC with undifferentiated carcinoma
PTC with squamous cell component
Combined PTC and medullary carcinoma
Cribiform carcinoma ^a

Risk factors

Radiation exposure, iodine intake, lymphocytic thyroiditis, hormonal factors and family history are putative risk factors for thyroid carcinoma.

Radiation exposure as a consequence of nuclear fallout is associated with papillary carcinoma. After the Chernobyl disaster, the effects of radiation exposure were most pronounced in children. It is not clear if this is because the thyroid is more susceptible to radiation damage in childhood, whether it is a reflection of the fact that children drank more contaminated milk, increasing their exposure to radioactive iodine, or both (Williams 2002). The predilection to radiation-induced injury seems to be closely linked to chromosomal rearrangement as opposed to intragenic point mutation as a mode of aberrant gene activation (Ciampi 2005).

Iodine is required for thyroid hormone organification. Papillary carcinoma is the most frequent type of thyroid cancer in iodine-sufficient regions (Delellis 2004, Harach 2002). Interestingly, in animal models, iodine supplementation causes experimental thyroid cancers to change from follicular to papillary morphology

Lymphocytic infiltration is frequently observed in papillary carcinoma, indicating that immunological factors might be involved in tumour progression. Recent molecular analyses indicate that chronic lymphocytic thyroiditis harbours potential precursor lesions of malignancy (Gasbarri 2004, Prasad 2004).

Most well-differentiated thyroid carcinomas manifest in patients who are 20–50 years of age, and the disease is 2–4 times more frequent in females than in males

(De Lellis 2004). These sex and age distributions of incidence indicate that female hormones might regulate thyroid carcinogenesis..

There is also a genetic component to thyroid follicular-cell-derived carcinoma, several susceptibility gene loci have been identified in other familial tumour syndromes that predispose to papillary carcinoma associated with papillary renal-cell carcinoma (1q21), clear-cell renal-cell carcinoma (3;8)(p14.2;q24.1)), and multinodular goitre (19p13.2) (De Lellis 2004,Eng 2000).

A variety of different genetic alterations, including rearrangements and point mutations have been implicated in the development of PTC. Targets of these genetic events include RET and TRK (rearrangements) and BRAF and RAS (point mutations). In general, rearrangements have been linked with radiation exposure while the origin of point mutations has remained unknown.

Chromosomal Rearrangement in PTC

TRK

The neurotrophic receptor-tyrosine kinase (NTRK1) gene is located on chromosome 1q22, and encodes the receptor for nerve growth factor. Similar to RET, NTRK1 undergoes oncogenic activation by chromosomal rearrangement (Greco 2004). NTRK1 rearrangements are considerably less frequently found in PTCs than are RET rearrangements (Bongarzone 1998).The prevalence of NTRK rearrangements is approximately 3% in post-Chernobyl PTCs (Rabes 2000).

RET

The RET protooncogene, which is located on chromosome 10q11.2 was first identified in 1985 (Takahashi 1985). It encodes a tyrosine receptor protein consisting of an extracellular domain with a ligand binding site, a transmembrane domain and an intracellular tyrosine kinase domain. RET is activated by interaction with a multicomponent complex that includes a soluble ligand family, the glial cell line-derived neurotrophic factors (GDNFs), and also a family of cell surface bound co-receptors, the GDNF family receptors (GFR α) (Li Volsi 2004). Ligand binding results in receptor dimerization leading to autophosphorylation of the protein on tyrosine residues and initiation of the signaling cascade. RET plays a critical role in the development and maturation of peripheral nerves, neuronal survival in the enteric plexus and in renal morphogenesis. The PTC oncogene was discovered on the basis of its ability to transform NIH3T3 cells (Fusco 1987, Grieco 1990). Subsequent studies demonstrated that PTC was a novel form of RET (RET/PTC) resulting from rearrangement of the 3' region of RET (which encodes the tyrosine kinase domain) and the 5' region of several genes that are expressed in normal follicular cells (Fusco 1987, Nikiforov 2002). The most common rearranged forms of RET are RET/PTC1 and RET/PTC3, resulting from paracentric inversions of the long arm of chromosome10, and RET/PTC2, resulting from a 10/17 reciprocal translocation involving R1a on17q23. More than 10 additional

types of RET rearrangements, occurring primarily in radiation-induced tumors, have been described but their frequencies are low (Nikiforov 2002). The role of RET/PTC in the development of PTC has been demonstrated convincingly in transgenic mice with targeted overexpression of RET/PTC1 and RET/PTC3. These animals develop tumors that are similar in many aspects to human PTCs (Santoro 1996). Additionally, Fischer and coworkers (Fischer 1998) have duplicated many of the nuclear characteristics of PTC in cultured follicular cells transfected with RET/PTC1. The frequency of RET rearrangements varies widely according to the methods of detection and to geographic/environmental factors (Nikiforov 2002, Tallini 2001). The frequency of rearrangements in the adult population in the U.S. is approximately 30–40%. In recent studies, RET rearrangements have emerged as the second most common genetic abnormality found in PTCs. RET/PTC1 and RET/PTC3 account for 60–70% and 20–30% of cases, respectively, while RET/PTC2 has been implicated in approximately 10% of cases. RET rearrangements are particularly common in tumors from pediatric patients (50–60%) and in patients exposed to accidental/therapeutic radiation during childhood (60–70%). Recent studies have suggested that spatial contiguity of RET and H4 may provide a structural basis for the generation of RET/PTC1 rearrangements by allowing a single radiation tract to produce a double strand break in each gene at the same site in the nucleus (Nikiforova 2000).

The RET/PTC1 rearrangement is more common in classic PTCs, papillary microcarcinomas, and the diffuse sclerosing variant than in other subtypes. RET/PTC3, on the other hand, has been associated with the solid variant. The overall prevalence of RET/PTC rearrangements appears to be lower in the follicular variant of PTC than in PTCs of classic type (Sobrinho-Simoes 2005, Nikiforov 2002, Andeniran 2006).

Genetic alterations in PTC

BRAF

The RAF proteins are serine/threonine protein kinases that play critical roles in cell proliferation, differentiation, and apoptosis by signaling along the mitogen-activated protein kinase pathway (MAPK) (Davies 2002, Rajagopalan 2002). Mammalian cells express three isoforms of RAF threonine kinase that have been designated ARAF, BRAF, and CRAF. BRAF is expressed at highest levels in hematopoietic cells, neurons, and testis, and is the predominant isoform in thyroid follicular cells. Among the isoforms of RAF kinase, BRAF appears to be the most potent activator of the MAPK pathway. BRAF mutations have been identified in approximately two-thirds of malignant melanomas and in a smaller proportion of colorectal and ovarian carcinomas (Davies 2002). The most common mutation results in a thymidine to adenine transversion at nucleotide position 1799 (originally thought to be 1796) with a valine to glutamate substitution at residue 600 (V600E). An identical mutation was initially found in 29% of papillary carcinomas but subsequent studies have demonstrated the mutation in 40–70% of the tumors (Kimura 2003, Cohen

2003, Xu 2003, Soares 2004, Fukushima 2003, Trovisco 2004, Trovisco 2006, Ciampi 2005). There is no evidence of BRAF mutation in benign or malignant follicular tumors, including oncocytic variants. BRAF mutations have been associated with conventional PTC, tall cell subtypes, oncocytic PTC, and microcarcinomas but only uncommonly with the follicular variant (Xing 2005). Trovisco reported BRAF (V600E) mutations in a series of uncommon PTC variants, including the Warthin-like (75%) and oncocytic (54%) variants. A different type of BRAF mutation (K601E) has been detected in a single case of follicular adenoma and in 4 of 54 (7%) cases of the follicular variant of PTC (Trovisco 2005). There is a substantial body of data to indicate that BRAF mutational status is a significant predictor of poor clinical outcome. In the study of Xing and coworkers involving 219 patients with PTC, there was a significant association with extrathyroidal invasion ($P < 0.001$), lymph node metastasis ($P < 0.001$), and advanced tumor stage III/IV ($P < 0.001$) at initial surgery (Xing 2005). BRAF mutations have also emerged as independent predictors of recurrence in patients with stage I/II disease ($P = 0.002$). These findings indicate that BRAF mutation may be a useful molecular marker to assist in risk stratification for patients. Approximately 15% of poorly differentiated thyroid carcinomas and a significantly higher proportion of undifferentiated/anaplastic carcinomas harbor BRAF mutations (Nikiforova 2003, Soares 2004). Moreover, BRAF mutations occur more commonly in undifferentiated or anaplastic carcinomas with a papillary component than in those without a concurrent papillary component. These findings suggest that undifferentiated or anaplastic thyroid carcinomas may progress from BRAF-positive papillary tumors. This hypothesis is strengthened by observations that targeted expression of BRAF^{V600E} in thyroid cells of transgenic mice results in the development of papillary carcinomas that undergo dedifferentiation (Knauf 2005). BRAF mutations are uncommon in radiation-induced PTCs; however, Ciampi and coworkers have reported rearrangement via paracentric inversion of chromosome 7q resulting in AKAP9-BRAF fusion (Ciampi 2005). The AKAP9 was found in 3 of 28 (11%) tumors that developed 5–6 years after radiation exposure from the Chernobyl accident but in none of 64 that developed 9–12 years after exposure.

RAS

Members of the RAS family are signal-transducing proteins that share properties with the G-proteins. While point mutations in H-RAS, K-RAS, and N-RAS have been described in many tumor types, they are uncommon in papillary carcinomas of conventional type with an overall frequency of less than 10% (Namba 1990, Capella 1996). In contrast, the frequency of mutations in the follicular variant of PTC is high. Adeniran and coworkers reported that 14 of 14 follicular variants of PTC (FVPTC) had RAS mutations with 10 involving N-ras (codon 61) and 4 involving H-ras (codon 61), (Adeniran 2006). In a comparison of FVPTC and conventional PTC, Di Cristofaro and coworkers demonstrated RAS mutations in 6/24 (25%) of cases of FVPTC but

in no cases of conventional PTC (Di Cristofaro 2006). BRAF mutations and RET rearrangements were found in 1/13 (7.6%) and 5/12 (41.7%), respectively, in FVPTC. Corresponding values for BRAF and RET rearrangements were 3/10 (30%) and 5/11 (45%) in conventional PTCs. Based on these findings, the authors concluded that RAS mutations correlated with follicular differentiation while RET activation was associated with papillary nuclei but not with papillary architecture. The genotype of FVPTC, therefore, is closer to that of follicular adenomas and carcinomas than to conventional PTC. These findings suggest that the FVPTC may occupy an intermediate position between follicular tumors and classic PTC.

1.4 Transcription factor cAMP response element-binding protein CREB

The cAMP response element-binding protein (CREB) was identified almost 20 years ago. Since then, CREB has become one of the most extensively studied transcription factors. This protein belongs to a class characterized by the ability to bind to the consensus sequence TGACGTCA(CRE) (Josselyn SA 2005, Carlezon WA 2005, Dolmetsch RE 2001) and contain a leucine zipper responsible for DNA binding (basic region) and for dimerization (leucine zipper region) of the proteins. CREB can form homodimers or heterodimers with other members of the ATF family, including ATF1 and CREM. However, heterodimerization of CREB with other members of the ATF family decreases its stability and CRE (cAMP Responsive Element) binding affinity (Johannessen M 2004). The cAMP/CREB signaling pathway has been strongly implicated in the regulation of a wide range of biological functions such as growth factor-dependent cell proliferation and survival, glucose homeostasis, spermatogenesis, circadian rhythms and the synaptic plasticity. The richness of CREB signaling is greatly increased by its responsiveness to multiple intracellular signal transduction cascades and the potential for this family of transcription factors to induce and suppress gene expression.

It is well known that numerous signals, not only the cAMP signal, but also Ca²⁺, cellular stresses and cell cycle systems, regulate CREB activity in a phosphorylation-dependent manner. The crucial event in the activation of CREB is the phosphorylation of Ser133 in KID (Kinase-Inducible Domain). This domain includes several consensus phosphorylation sites for a variety of kinases like PKA (Protein Kinase-A), PKC (Protein Kinase-C), CSNK (Casein Kinases), CaMKs (Calmodulin Kinases), GSK3 (Glycogen Synthase Kinase-3) and p70S6K that can either increase or decrease the activity of CREB. Ser133 phosphorylation of CREB can be caused by electrical activity, growth factors, Neurotransmitter or Hormone action on GPCR (G-Protein-Coupled Receptors), or by Neurotrophin effects on RTKs (Receptor Tyrosine Kinases) (Mayr B 2001). Upon stimulation of cellular GPCR (G-Protein-Coupled Receptors) and Growth Factor Receptors, AC (Adenylate Cyclase) is activated by G-proteins leading to increases in cAMP. This in turn activates PKA by dissociating the regulatory (PKAR) from the catalytic (PKAC) subunits. In the basal state, PKA resides in the cytoplasm as an inactive heterotetramer of paired regulatory and

catalytic subunits. Induction of cAMP liberates the catalytic subunits, this translocate to the nucleus, where phosphorylates CREB at SER 133 and lead to the recruits the transcriptional coactivators CBP (CREB Binding Protein) and p300. CBP/p300 stimulates gene expression by interacting with components of the general transcriptional machinery or by promoting the acetylation of specific lysine residues in nucleosomes located near transcriptionally active promoters thus creating access to the gene for the basal transcriptional machinery. The basal transcriptional machinery includes TBP (TATA-binding protein), TFIIB (Transcription Factor-II-B), and RNA Pol II (RNA Polymerase-II) (Mayr 2001). The accumulation of cAMP in response to activation of GPCR also induces PLC-Gamma (Phospholipase-C-Gamma) that catalyzes the formation of DAG (Diacylglycerol), a PKC activator through PI (Phosphatidylinositols). PI3K (Phosphoinositide-3kinase) is responsible for activation of Akt/PKB (Protein Kinase-B) which directly or indirectly affects CREB (Figure 3).

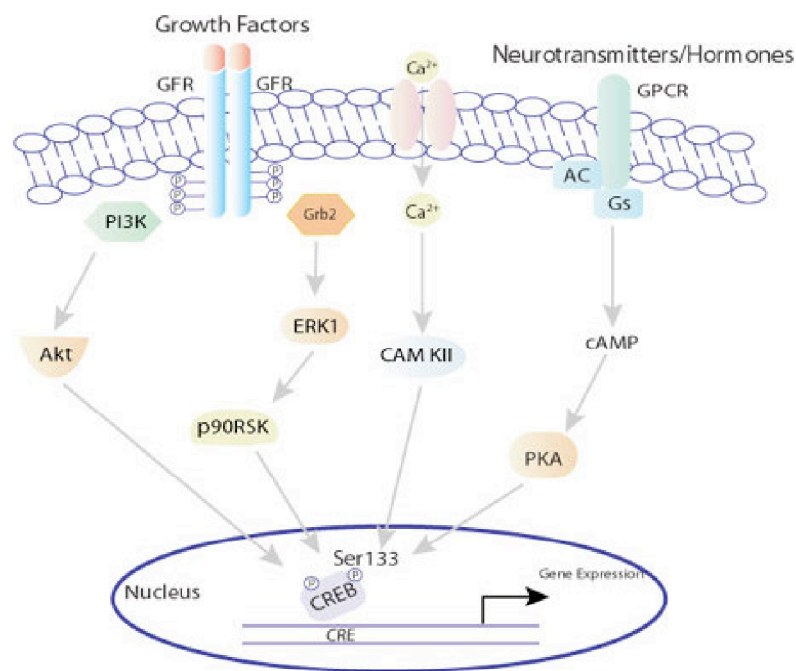


Figure 3 CREB Pathway

Regulated activation of CREB has a significant impact on cellular growth, proliferation and survival. To overturn the cellular control of these processes, tumor cells have developed various mechanisms to achieve constitutive activation of CREB, including gene amplification, chromosome translocation, interaction with viral oncoproteins, and inactivation of tumor suppressor genes. These mechanisms converge on the phosphorylation of CREB at Ser 133 promoting its association with CREB-binding protein CBP or its paralogue p300 and inducing transcriptional activation. The characterization of putative cofactors that modulate complex formation in a stimulus-dependent manner should provide new insights into cancer process.

1.5 H4

In the various RET/PTC oncoproteins, little is known about the normal role of the 5' fusion partners. Some common features such as constitutive expression and the presence of dimerization domains have been observed for all the RET-fused genes identified so far. The ubiquitously expressed promoters of the 50 - fused sequences are responsible for the ectopic expression of RET in epithelial thyroid follicular cells, which do not normally express this protooncogene. Although this indicates that disruption of the normal regulation of the RET kinase is critical to the transforming properties, less is known about whether disruption of the normal function of the 5' partner genes might also have an important role. To address this point, the identification of the normal physiological function of the heterologous RET fusion partners is required. Therefore, we have characterized the product of the first and most frequently observed RET-fused gene, H4(D10S170).

H4(D10S170) gene product is an ubiquitously expressed 55 kDa nuclear and cytosolic protein, phosphorylated by extracellular signal-regulated protein kinase following serum stimulation with no significant homology to known genes (Grieco et al., 1994; Celetti et al., 2004).

The 60 amino acid fragment of the H4 coiled-coil domain included in the RET/PTC1 product has been shown to be necessary for homo-dimerization, constitutive activation and transforming ability of the oncoprotein (Tong et al., 1997; Jhiang, 2000). New rearrangements involving H4(D10S170) gene have been reported (Kulkarni et al., 2000; Schwaller et al., 2001; Puxeddu et al., 2005), suggesting that H4 gene has high susceptibility for recombination.

Even though the function of H4(D10S170) wild type (wt) has not been clarified, Celetti et al. reported the involvement of this gene in apoptosis and the ability of its truncated mutant H4(1-101), which corresponds to the portion of H4 included in RET/PTC1, to act as dominant negative on the wt H4(D10S170)-induced apoptosis (Celetti et al., 2004). The 90% papillary thyroid tumours, that harbours the RET/PTC1 rearrangement, has lost the expression of the normal unrearranged H4(D10S170) allele. Thus, it is possible that the transforming potential of RET/PTC1 is not limited to the RET tyrosine kinase activation, but it may also involve the disruption of the H4 function.

Merolla et al. demonstrated the potential role of H4 in DNA damage signalling pathways (Merolla 2007). The most important process for the survival of a cell following ionizing radiations is the repair of DNA double-strand breaks (DSBs) (Leskov et al., 2001). The product of the ataxia telangectasia mutated (ATM) gene, a major regulator of cellular responses to DNA damage, plays an essential role in maintaining genome stability (Kastan and Lim, 2000; Bakkenist and Kastan, 2003; Shiloh, 2003; Lee and Paull, 2004).

Merolla et al. (2007) show that H4(D10S170) protein is phosphorylated by ATM kinase after etoposide treatment or ionizing irradiation exposure and provide the first evidence of a functional relationship between H4(D10S170) gene product and ATM kinase. They suggest that H4 (D10S170) is involved in cellular response to DNA damage ATM-mediated, and the impairment of H4 (D10S170) gene function might have a role in thyroid carcinogenesis.

2. Aims of the study

Papillary thyroid carcinoma (PTC) is the most common thyroid malignancy and the biological behaviour of PTC varies widely from indolent microcarcinomas, growing slowly with little or no invasion, to invasive tumours that metastasize and can cause death.

Most human thyroid papillary carcinomas are characterized by rearrangements of the RET protooncogene with a number of heterologous genes, which generate the RET/papillary thyroid carcinoma (PTC) oncogenes.

RET/PTC rearrangements are specific for thyroid carcinomas of papillary histotype and are considered early events in the tumorigenesis process because they are frequently found in clinically silent small PTCs (Viglietto *et al.*, 1995).

In the various RET/PTC oncoproteins, little is known about the normal role of the 5' fusion partners. Some common features such as constitutive expression and the presence of dimerization domains have been observed for all the RET-fused genes identified so far. The ubiquitously expressed promoters of the 5' - fused sequences are responsible for the ectopic expression of RET in epithelial thyroid follicular cells, which do not normally express this protooncogene. Although this indicates that disruption of the normal regulation of the RET kinase is critical to the transforming properties, less is known about whether disruption of the normal function of the 5' partner gene might also have an important role. To address this point, the identification of the normal physiological function of the heterologous RET fusion partners is required. Therefore, we have characterized the product of the first and most frequently observed RET-fused gene, H4(D10S170). The 90% papillary thyroid tumours, that harbours the RET/PTC1 rearrangement, has lost the expression of the normal unarranged H4 (D10S170) allele. The loss of the normal allele of this gene might result in growth advantage in tumour progression.

We used functional proteomics approach to elucidate biological function of H4.

The association of an unknown protein with partners belonging to a specific protein complex involved in a particular process would in fact be strongly suggestive of its biological function (Gavin 2002, Ho 2002). The proteomics approach showed some proteins interacting with H4.

Among them, we selected the CREB1 protein because of its relevance in thyroid tumour biology; in fact thyroid cells are dependent on TSH for growth and differentiation (Kimura 2001). TSH activates its specific receptor in thyroid cells and induces cAMP pathway.

Regulated activation of CREB has a significant impact on cellular growth, proliferation and survival. To overturn the cellular control of these processes, tumor cells have developed various mechanisms to achieve constitutive activation of CREB, including gene amplification, chromosome translocation, interaction with viral oncoproteins, and inactivation of tumor suppressor genes. These mechanisms converge on the phosphorylation of CREB at Ser 133

promoting its association with CREB-binding protein CBP or its paralogue p300 and inducing transcriptional activation. The characterization of putative cofactors that modulate complex formation in a stimulus-dependent manner should provide new insights into cancer process. Thus, once demonstrated the interaction between H4 and CREB1, we proceeded in investigating the functional consequences of this interaction.

3. Materials and Methods

3.1 Cell cultures and treatments and transfection.

Hela and TPC1 cells were maintained respectively in RPMI and in Dulbecco's modified Eagle's medium (DMEM), supplemented with 10% foetal calf serum (GIBCO-BRL, Life Technologies, Gaithersburg, Maryland, United States of America), 10 mM glutamine (Gibco BRL), 100 µg of ampicillin/ml, and 32 µg of gentamicin/ml (Sigma Chemical Co). Cells were grown at 37°C in a humidified CO₂ atmosphere.

TSA (Sigma) was dissolved in ethanol and added to the culture medium at 300 nM. A corresponding volume of ethanol was added to control untreated cells. TSA treatments were performed for 24 h after transfection.

Hela cells were transfected with plasmids by Fugene reagent (Roche).

TPC1 cells were transfected with plasmids by Arrestin (OpenBiosystem), as suggested by the manufacturer.

3.2 Expression constructs

The expression plasmid H4WT was constructed by inserting in the BamHI-XhoI sites of pcDNA4ToA/myc-his (Invitrogen) the PCR fragment corresponding to the entire coding sequence (nt1-1791).

The expression plasmid CREB1 is pCMVSPORT6 CREB1 (Invitrogen).

The pGST-H4 wt construct was obtained amplifying by polymerase chain reaction (PCR) the entire coding sequence (nt1-1791) and then subcloned in the BamHI-EcoRI restriction sites of pGEX2TK (Amersham, Pharmacia Biotech, Buckinghamshire,UK).

3.3 Transactivation assay.

In the luciferase transactivation assay HeLa cells were transiently transfected with the reporter construct in which the luciferase gene was driven by a fragment containing three sites CRE and normalized with the use of a co-transfected Renilla construct (kindly provided by Fanciulli). Cotransfections were carried out in the presence of 200 ng of reporter CRE Luc construct and 500 ng of Renilla construct and of 2µg of pSPORT6CMV-CREB1, pcDNA4ToA, pcDNAMyc-His-tagged-H4, or pSPORT6CMV-CREB1 with or without the indicated amounts of pcDNA4TOA-H4 constructs. Luciferase and Renilla activities were measured with the dual-luciferase reporter assay kit (Promega) and normalized to the wild-type promoter activity detected in mock-transfected (pcDNA4ToA) or untreated cells.

3.4 In vitro proteins translation and pull down assay.

GST fusion proteins were produced in Escherichia coli BL21 cells. Stationary phase cultures of E. coli cells transformed with the plasmid of interest were diluted 5–400 ml in LB with ampicillin (100 mg/ml), grown at 30°C to an OD 600 of 0.6 and induced with 0.1mM IPTG. After an additional 2 h at 30°C, the

cultures were harvested and resuspended in 10 ml of cold PBS (140 mM NaCl, 20mM sodium phosphate (pH 7.4)), 1mM phenylmethylsulfonyl fluoride (PMSF) and protease inhibitors (Boehringer). The cells were broken by French Press. For the GST proteins, the supernatant was then incubated at 4°C for 1 h with 250 ml of glutathione-Sepharose beads (Amersham Pharmacia Biotech). The resin was washed with PBS and protease inhibitors. The recombinant proteins were eluted with a buffer containing PBS, 10mM reduced glutathione, and 10% (v/v) glycerol. The recombinant proteins were subjected to *in vitro* protein-protein binding. The proteins were incubated with total cellular extracts (TCEs) in NETN buffer (20mM Tris-HCl, pH 8.0, 100mM NaCl, 1mM EDTA, and 0.5% Nonidet P-40) for 1 h at 4°C. The resins were then extensively washed in the same buffer. The bound proteins were separated by SDS-PAGE, and analysed by Western blotting.

3.5 Total protein extracts , Western blotting, and immunoprecipitation assay

Cells were washed twice in phosphate-buffered saline and lysed in lysis buffer (50mM Tris Hcl pH 7.5, 5mM EDTA, 300mM NaCl, 150mM KCl, 1mM dithiothreitol, 1% Nonidet P40, and a mix of protease inhibitors) for 10 minutes in

ice Lysates from adherent cells were obtained by centrifuging cells at 12,000 g for 15 min at 4°C. The supernatants were collected and protein concentration in cell

lysates was determined by Bio-Rad Protein Assay (Bio-Rad, Richmond,CA)

Western blotting

Protein extracts and immunoprecipitated pellets were separated by SDS-PAGE, and then transferred onto Immobilon-P Transfer membranes (Millipore) Membranes were blocked with 5% non-fat milk proteins and incubated with Abs at the appropriate dilutions. The filters were incubated with horseradish peroxidase-conjugated secondary Abs and the signals were detected with ECL Western blotting procedure were carried out as reported elsewhere (16). To ascertain that equal amounts of protein were loaded, the western blots were incubated with antibodies against the α -tubulin protein (Sigma). Membranes were then incubated with the horseradish peroxidase-conjugated secondary antibody (1:3000) for 60 min (at room temperature) and the reaction was detected with a western blotting detection system (ECL) (GE Healthcare).

Immunoprecipitation assay

For co-immunoprecipitation experiments, TCE were incubated with protein A-sepharose or G sepharose beads (Amersham) for 1 h at 4 C, then samples were centrifugated to 2000 rpm to eliminate beads and incubated overnight with Abs and then supplemented with protein A-sepharose or G sepharose beads (Amersham). After 1 h, the beads were collecte and washed five times with lysis buffer, and boiled in Laemmli sample buffer for immunoblotting analysis.

Protein extracts and immunoprecipitated pellets were separated by SDS-PAGE, and then transferred onto

Immobilon-P Transfer membranes (Millipore) Membranes were blocked with 5% non-fat milk proteins and incubated with Abs at the appropriate dilutions. The filters were incubated with horseradish peroxidase-conjugated secondary Abs, and

the signals were detected with ECL. The Abs used for immunoprecipitation and for western blot were:

home made anti-H4 are polyclonal Ab raised against a synthetic peptide located in Proline-rich region; antiHDAC1(06720) (Upstate Biotechnology) ; anti-cyclin D3 C-16, and anti-cyclin B1 GNS1, anti-cyclin E HE12, anti-cyclin A sc751, anti-cdc2 M2, antiCreb1, anti-CDK4 C22, antiMyc(E910) , anti-ATF1, anti-ATF2 , anti-ATF3, antiCREM, anti-CREB2 (Santa Cruz Biotechnology Inc.); and anti-cdc2 Ab-1 (Calbiochem) anti pCREB (Cell Signaling). Anti tubulin (Santa Cruz Biotechnology) was used to equalize the amount of proteins loaded. Bound antibodies were detected by the appropriate secondary antibodies and revealed with the Amersham enhanced chemiluminescence system.

3.6 Nuclear extracts preparation.

Cells were washed twice in phosphate-buffered saline and resuspended in 3 volumes of a solution containing 10 mM HEPES pH 7.9, 10 mM KCl, 1.5 mM MgCl₂, 0.1 mM EGTA, 0.5 mM DTT (homogenization solution). The cells were disrupted by passage through a 26-gauge needle. Nuclei were collected by centrifugation at 1500 r.p.m. and resuspended in a 1.2-volume of extraction solution containing 10 mM HEPES pH 7.9, 0.4 M NaCl, 1.5 mM MgCl₂, 0.1 mM EGTA, 0.5 mM DTT, 5% glycerol, to allow elution of nuclear proteins by gentle shaking at 4°C. Nuclei were pelleted again by centrifugation at 12 000 r.p.m. and the supernatant was stored at -70°C until used. The protease inhibitors leupeptin (5 mM), aprotinin (1.5 mM), phenylethylsulfonylfluoride (2 mM), pepstatin A (3 mM), and benzamidine (1 mM) were added to both homogenization and extraction solutions. Protein concentration was determined by the Bradford protein assay (BioRad).

3.7 Electrophoretic mobility shift assay (EMSA) and supershift assay.

For gel shift analysis, we prepared nuclear extracts following the method of Dignam, et al (1). CREB Consensus oligonucleotide probe are ³²P labeled (TransCruz™ Gel Shift Oligonucleotides) with ³²P]-ATP to 50,000 cpm/ng by using polynucleotide kinase. Binding reaction mixtures(20 ul) are incubate for 20 minutes at room temperature and contain 2,5fmol DNA probe(20000 cpm) and 2,5 µg nuclear extract and 1 µg poly dI-dC to inhibit non specific binding of the labeled probe to nuclear extract protein, in 10 mM Tris pH7.5, 50 mM NaCl 1 mM dithiothreitol (DTT), 1 mM EDTA, 5% glycerol. The protein-DNA complexes were resolved by native PAGE(8% gel) in 0,5xTris/borate/EDTA and visualized by autoradiography.

To supershift analysis, assays were performed as described above with the expectation that antibody (2 ug) is normally added 4 h prior to addition of labeled oligonucleotide probe.

3. 8 RNA isolation

Total RNA was extracted by cell cultures using the RNeasy mini kit (Qiagen, Valencia, CA) according to the manufacturer's instructions. The integrity of the RNA was assessed by denaturing agarose gel electrophoresis.

3.9 Reverse transcriptase and Real Time PCR analysis

Reverse transcription

1 µg of total RNA of each sample was reverse-transcribed with the QuantiTect® Reverse Transcription (QIAGEN group) using an optimized blend of oligo-dT and random primers according to the manufacturer's instructions.

Selection of primers and probes for quantitative PCR

To design a qPCR assay we used the Human ProbeLibrary™ system (Exiqon, Denmark). Briefly, using locked nucleic acid (LNA™) technology, Exiqon provides 90 human prevalidate TaqMan probes of only 8-9 nucleotids that recognize 99% of human transcripts in the RefSeq database at NCBI. The free ProbeFinder assay design software, which is an integrated part of the package, is available on the web site www.probelibrary.com. All fluorogenic probes were dual-labeled with FAM at 5' end and with a black quencher at the 3' end. I chose the best probe and primers pair, to amplify a fragment for real-time PCR of AREG mRNA, entering its accession number (NM_AY442340.1) on the assay design page of the ProbeFinder software. ProbeFinder generated an intron-spanning assay identifying the exon-exon boundaries within submitted transcript. Based on these data, the software provided us various solutions. We chose an amplicon of 110 nucleotides. The number of probe was "human 54" (according to the numbering of Exiqon's Human ProbeLibrary kit) and the primer sequences were: AREG forward 5'-gtgggcagatcccttgag-3'; AREG reverse 5'-ctgtcaccattgtactcagctaac-3'.

The same procedure was used to choose both probe and primers for the housekeeping gene G6PD, accession number X03674. The ProbeFinder provided us various solutions for G6PD, as well as AREG transcript. We opted for an amplicon of 106 nucleotides scattered among 3th and 4th exons. The number of probe was "human 05" (according to the numbering of Exiqon's Human ProbeLibrary kit) and the primer sequences were: G6PD forward 5'-acagagtgagcccttcttcaa-3'; G6PD reverse 5'-ggaggctgcatcgtact-3'.

Real-time RT-PCR

Relative Quantitative TaqMan PCR was performed in Chromo4 Detector, MJ Research in 96-well plates using a final volume of 20 µl. For PCR we used 8 µl of 2,5x RealMasterMix™ Probe ROX (Eppendorf AG, Germany) 200 nM of each primer, 100 nM probe and cDNA generated from 50 ng of total RNA. The conditions used for PCR were 2 min at 95°C and then 45 cycles of 20 sec at 95°C and 1 min a 60°C. Each reaction was performed in duplicate.

To calculate the relative expression levels we used the 2^{-DDCT} method (5).

3.10 HDAC activity.

Hela cells were transiently transfected with Myc-His-pcDNA4ToA or Myc-His-H4 WT plasmids and were used to assay the HDAC activity. The total protein extracts (30 ug) were incubated with 5 μ l of [3 H]acetate-labeled histone H4 (1.8 nCi/ μ g) in 200 μ l of activity buffer (25 mM Tris-HCl [pH 7.5], 10% glycerol, 1 mM EDTA, 125 mM NaCl) ON at 37°C. The reaction was stopped by the addition of 50 μ l of

1 N HCl-0.4 M acetate and the released [H3]acetate was extracted with 600 μ l of ethyl acetate. After centrifugation, a 100 μ l aliquot of the supernatant was counted in 5 ml of scintillation cocktail. All experiments were carried out three times, and samples were assayed in duplicate.

3.11 Chromatin immunoprecipitation (ChIp) and Re-ChIp assays

Chromatin immunoprecipitation

TPC1 cells were cultured in Dulbecco's modified Eagle's medium supplemented with 10% fetal bovine serum (growth medium). Cells (5×10^5) were plated in 10 mm plates 24 h before transfection and then transiently transfected with pcDNA4ToAMYC His-H4WT and pcDNA4ToAMYC His (5 μ g of each plasmid) by Arrestin (OpenBiosystem), according to the manufacturer's protocol. After transfection (48 h), transfected cells were fixed by adding formaldehyde

directly to culture medium to a final concentration of 1%, and incubated for 10 min at 37 °C. The reaction was stopped with glycine 0.125M for 5 min. The fixed cells were scraped with ice-cold PBS containing protease inhibitors (1 mM PMSF and 1 g/ml leupeptin), pelleted for 4 min at 700 g at 4 °C, and resuspended in 300 μ l of SDS lysis buffer (1% SDS, 10 mM EDTA and 50 mM Tris/HCl, pH 8.1) for 10 min on ice. The lysates were sonicated to reduce DNA length between 200 and

1000 bp. Debris was removed by centrifugation for 10 min at 9800 g at 4 °C, and the supernatant fraction diluted 10-fold in chromatin immunoprecipitation dilution buffer (0.01% SDS, 1.1% Triton X-100, 1.2 mM EDTA, 16.7 mM Tris/HCl, pH 8.1,

150 mM NaCl, 1 mM PMSF and 1 g/ml leupeptin). A portion of this chromatin solution was kept as a template for PCR positive control. To reduce non-specific background, the chromatin solution was pre-cleared with 40 μ l of salmon sperm

DNA Protein A agarose slurry or salmon sperm DNA Protein G agarose slurry for 3h at 4 °C with agitation. Beads were pelleted by brief centrifugation at 1800 g, and the supernatant fraction was collected. Immunoprecipitations were performed with 2 μ g of HDAC1 (Upstate Biotechnology) polyclonal antibody, CREB1 (Santa Cruz) polyclonal antibody and anti-H4 (polyclonal antibody raised against a synthetic peptide located in the proline rich region) incubated overnight at 4 °C with rotation. Equal volumes of the supernatant fractions

were saved for a no-antibodies control, and incubated with 3 μ l of normal rabbit or normal mouse serum. Immune complexes were collected with 40 μ l of salmon sperm DNA/Protein A agarose slurry or salmon sperm DNA/Protein G agarose slurry, for 3 h at 4 °C with rotation. Beads were pelleted by centrifugation and washed for 3 min on a rotating platform with 1 ml of each of the listed buffers: low-salt immune complex wash buffer (0.1% SDS, 1% Triton X-100, 2 mM EDTA, 20 mM Tris/HCl, pH 8.1, and 150 mM NaCl), high-salt immune complex wash buffer (as for the low-salt buffer but with 500 mM NaCl), LiCl immune complex wash buffer (0.25 M LiCl, 1% Nonidet P-40, 1% deoxycholate, 1 mM EDTA and 10 mM Tris/HCl, pH 8.1) and 1^x Tris/EDTA (two washes). Immune complexes were eluted by adding 200 μ l of elution buffer (1% SDS and 0.1 M NaHCO₄) to pelleted beads, vortexing briefly to mix and incubating at room temperature for 15 min with rotation. Beads were pelleted, and the eluates carefully transferred to other tubes. This step was repeated a second time and eluates were combined. I added 20 μ l of 5 M NaCl to the combined eluates, and cross-links were reversed by incubating at 65 °C for 4 h. After incubation, 10 μ l of 0.5 M EDTA, 20 μ l of 1 M Tris/HCl, pH 6.5, and 20 μ g of proteinase K were added to the eluates, and incubated for 1 h at 45 °C. The DNA was recovered by phenol/chloroform extraction and ethanol precipitation. Pellets were washed with 1 ml of 70% ethanol, air dried and resuspended in 50 μ l of sterile double-distilled water. I used 5 μ l of the resuspended DNA as a template for the PCR. PCR reactions were carried out by standard procedures, for a number of cycles optimized to ensure product intensity within the linear phase of amplification. The PCR products were separated on a 2% agarose gel, stained with ethidium bromide. Primers sequence of AREG promoter including the CRE site are :
p AREG F 5'-TCAGCGAA TCCTTACGCA -3' and
pAREG R 5'- TGC CGC TTT ATA GGC TCA -3'
and the primers sequence of GAPDH are:
h GAPDH pF 5'-GTATTCCCCCAGGTTTACATG-3'
h GAPDH pR 5'- TTCTCCATGGTGGTGAAGAC-3'

Re-Chip assay

For Re-ChIP experiments, complexes were eluted by incubation for 30 min at 37°C

in 250 μ l of Re-ChIP elution buffer (2 mM DTT, 1% Triton X-100, 2 mM EDTA, 150 mM NaCl, 20 mM Tris-HCl, pH 8.1) and then diluted 4-fold in Re-ChIP dilution buffer (1% Triton X-100, 2 mM EDTA, 150 mM NaCl, 20 mM Tris-HCl, pH 8.1) and subject again to the ChIP procedure.

3.12 Mouse H4 Gene Targeting and Mating

H4 knockout mouse was performed by Murinus GmbH. Briefly, to clone the mouse *H4* genomic locus, a phage library of mouse 129/Sv genomic DNA (Stratagene, La Jolla, California) was screened using a mouse *H4* cDNA as a probe, which was obtained by cross-hybridization experiment with human *H4*

cDNA. A targeting vector was constructed from subcloned genomic fragments. For the selection of targeted clones, a neomycin-resistance (*neo*) cassette was placed in the opposite transcriptional orientation to the endogenous *H4* gene. The final product consists of a 5' genomic fragment (1,66kb) containing exon 1, the *neo* cassette (1.7 kb) and a downstream *H4* genomic fragment (5,73kb). Thus, a ~12 kb *H4* genomic region containing exon 2 was replaced with the *neo* cassette vector.

Linearized targeting vector DNA was introduced by electroporation into 129/Sv embryonic stem (ES) cells (incute Genomics). After G418 selection, genomic DNA of resistant clones was analyzed by Southern blot analysis. To generate chimeras, cells of targeted clones were injected into host blastocysts of C57BL/6J mice then transferred into uteri of pseudo-pregnant females. Male chimeras were mated with C57BL/6J females and F1 heterozygous progeny were intercrossed. Mice were genotyped for the *h4* deletion by PCR. Primers used for genotyping:

H4 ln3R1 5'-GGAGGCAGATGAGTTCCTAAGG-3'

NEO5'R 5'-CTAAAGCGCATGCTCCAGACTGCC-3'

H4U2 5'-CAGTAACACTTTATTCAAGAAAATCCAG-3'

3.13 Growth Rate

The cells (10^5 /dish) were plated in 60-mm plates and cultured in complete medium. They were counted every day for 10 consecutive days to extrapolate the growth curves.

3.14 Apoptosis detection

Apoptosis was evaluated by using annexin V-FITC staining technique. Briefly, MEFs cells were collected and annexin V-FITC stained by using a detection kit from Medical & Biological laboratories CO., LTD, Naka-ku Nagoya Japan according to the manufacturer's instructions. Fluorescence analysis was performed by a flow cytometer apparatus (Becton & Dickinson, Mountain View, CA) and the CELL QUEST analysis software. For each sample, at least 30,000 events were stored. Quadrant settings were based on the negative control. Each experiment was repeated at least three times.

3.15 Cell cycle analysis.

MEFs cells were analyzed for DNA content as described previously (Krishan 1975). Cells were collected and washed in PBS. DNA was stained with propidium iodide (50 µg/ml) and analyzed with a FACScan flow cytometer (Becton Dickinson, San Jose, CA) that was interfaced with a Hewlett-Packard computer (Palo Alto, CA). Cell cycle data were analyzed with the CELL-FIT program (Becton Dickinson).

3.16 MEFs culture

MEFs were derived from 12.5-day-old embryos as previously described (McCurrach and Lowe, 2001). Briefly, after removal of the head and internal

organs, embryos were rinsed with phosphate-buffered saline (PBS), minced, and resuspended in DMEM containing 10% FBS and 2 mM glutamine, and 100 IU/ml penicillin and 100 µg/ml streptomycin. Cell media and reagents were obtained from GIBCO-BRL. Cells from single embryos were plated into one 100 mm culture dish (Falcon) and incubated at 37°C in a 5% CO₂-humidified chamber. Plating after disaggregation of embryos was considered passage 0, and the first replating 3 days later was considered passage 1. Genotypes of MEFs were verified by PCR .

4. Results and Discussion

4.1 H4 binds CREB1

In order to determine the function of H4(D10S170) and establish its role in the pathogenesis of papillary thyroid tumour, it was decided to identify H4 interacting proteins using a proteomic assay. To this aim, the HeLa cells were transiently transfected with a V5-tagged-H4wt expression vector or empty vector and were immunoprecipitated the protein lysates with anti-V5 antibody. After SDS-page, single components of the immunoprecipitated complexes were analyzed by mass spectrometry. Among proteins interacting with H4 wt, we selected the CREB1 protein because of its relevance in thyroid tumour biology; in fact thyroid cells are dependent on TSH for growth and differentiation (Kimura 2001). TSH activates its specific receptor in thyroid cells and induces cAMP pathway.

The data of the proteomic assay were validated by binding study (pull down assay).

To this purpose, the H4(D10S170) cDNA insert was cloned in frame into bacterial expression GST plasmid (pGEX2T) to obtain GST- H4(D10S170) fusion protein. Then, GST-H4 was tested for the ability to bind CREB family proteins in vitro. Protein lysates from HeLa cells were incubated with GST-H4 or GST beads for 2 hours, then the bound proteins were separated by SDSPage and the gels were analyzed by Western Blot using the antibodies for the different CREB family proteins. As shown in fig 4, when western blot was performed for α ATF1, α ATF3, α CREM, α CREB2 no specific bands in the lane for GST and GST-H4 were detected; the western blot for α ATF2 shows an aspecific band in GST lane and a specific band for GST-H4, while the western blot for α CREB1 show a band in the lane for GST-H4 and no band in the lane for GST. The data of pull down assay confirmed a specific, direct physical interaction between H4(D10S170) and CREB1 and between H4(D10S170) and ATF2, but not with other CREB family proteins. My interest is focalized on CREB1 protein and the relation with H4.

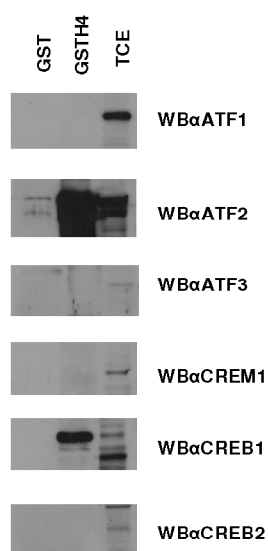


Figure 4 *In vitro* interaction between H4 and CREB1.

GST pull-down assays were performed between total cell extracts (TCEs) from HeLa cells and the GST or GST-H4 fusion protein. The bound complexes and TCEs were separated on SDS-PAGE and analysed by Western blotting with antibody for different proteins of CREB family (α ATF1, α ATF2, α ATF3, α CREM1, α CREB1, α CREB2)

To verify the H4/CREB1 interaction *in vivo*, HELA cells were transiently transfected with the Myc-His-tagged-H4 expression vector (pCMVH4). Protein lysates were immunoprecipitated with anti-H4 antibody and immunoblotted with anti-Myc and anti-CREB1 antibodies. As shown in Figure 5, I was able to detect the association between H4 and the endogenous CREB1 protein, demonstrating that H4 and CREB1 form complexes *in vivo*. The reciprocal experiment was performed immunoprecipitating with anti-CREB1 and revealing with anti-H4 antibody: it confirmed the interaction between the H4 and CREB1 proteins.

The negative control of immunoprecipitation was performed using an unrelated antibody.

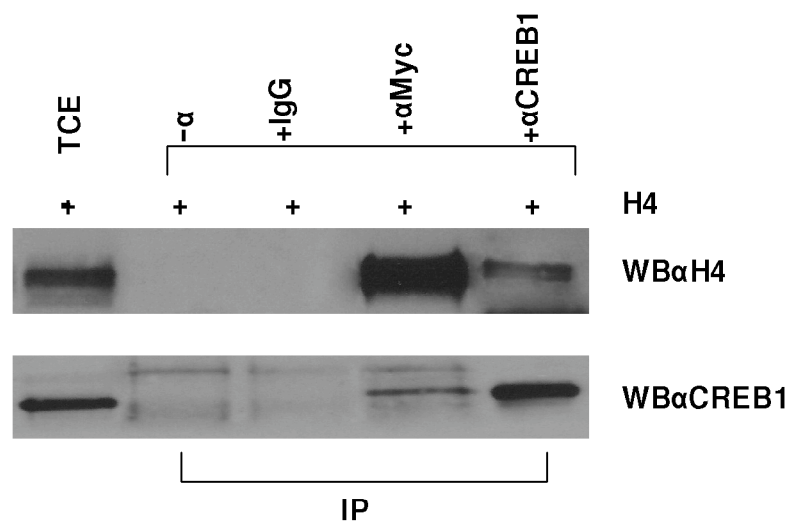


Figure 5 *In vivo* characterization of the H4/CREB1 interaction.

Hela cells were transfected with pCMVH4 vector. After 48 h, total cell extracts were prepared and equal amounts of proteins were immunoprecipitated with anti-myc or anti-CREB1 antibodies, the immunocomplexes analysed by Western blotting using the reciprocal antibodies (antiH4 and antiCREB1). The relative inputs are total cell extracts derived from Hela-transfected cells with the expression vector encoding H4. IgG indicates the negative control of immunoprecipitation using an unrelated antibody.

4.2 H4 inhibits the transcriptional activity of CREB1

Since H4(D10S170) interacts with CREB1, we investigated if the interaction between H4(D10S170) and CREB1 can be directly involved in transactivating activity of CREB1. To test this hypothesis, we studied the effect of H4(D10S170) on a reporter gene system in which the tandem three CRE universal sites are fused upstream to a luciferase cDNA in HeLa cells. HeLa cells were cotransfected with Luc reporter construct and Renilla construct and PCDNA 4ToA, pSPORT 6 CREB1, Myc-His-tagged-H4 or pSPORT 6 CREB1 and increasing amounts of Myc-His-tagged-H4. As shown in Figure 6, the CRELuc reporter construct basal activity is not modified by the expression of H4. The overexpression of CREB1 activated the reporter more than 2-fold whereas cotransfection of H4(D10S170) resulted in a decrease of CREB1 activation in a dose-dependent manner.

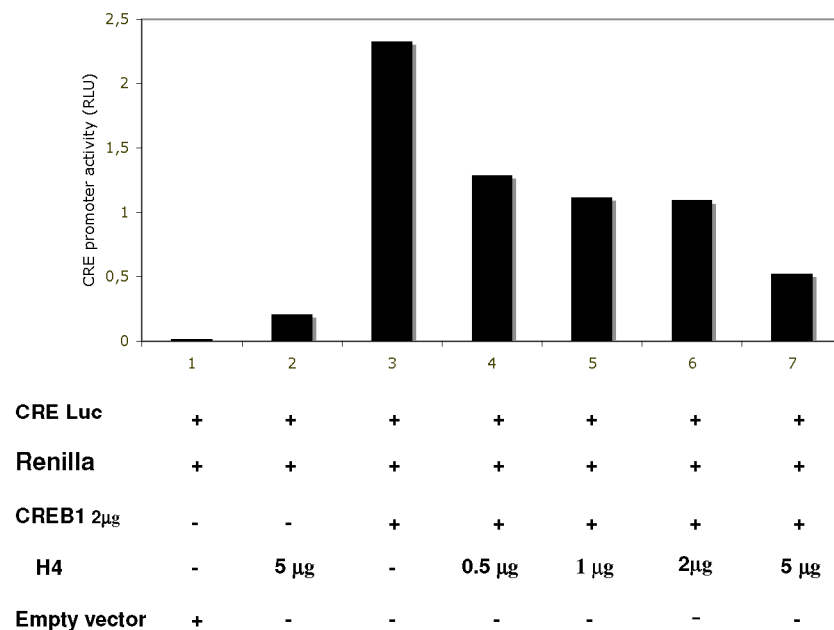


Figure 6 H4 reduces CREB1 transcriptional activity.

Luciferase assay performed using increasing amounts of H4 on CREB1 activity on the luciferase-reporter vector in HeLa cells. Cotransfections were carried out in the presence of 200ng of reporter construct and 500 ng of Renilla construct and of 5ug of H4 or 2ug of pCMVSPORT6-CREB1 with or without the indicated amounts of pCDNA4TOA-H4 constructs. All transfections were performed in duplicate and the data are means of five independent experiments. Empty vectors were used as control.

4.3 H4 reduces CREB1 target genes trascription

In order to confirm the Luciferase assay data, we evaluated the expression of CREB1 gene targets by Real Time PCR. We chose AREG gene, a CREB1 target gene with an antiapoptotic role in lung cells. The analysis was done in TPC1 cells, which harbours the RET/PTC1 rearrangement and have lost the expression of the normal unrearranged H4 allele. The cells were transfected with the Myc-His4ToA (pCMV) or Myc-His-tagged-H4 (pCMVH4) expression vector. After 24 hrs of starvation by serum the cells were treated with serum for 2 hr to activate the transcription and RNA was extracted. As reported in Figure 7, the expression of AREG increased in serum treated cells than untreated cells due to the activation of the cAMP pathway. In the TPC1H4 cells the expression was reduced compared to the control, with a fold change ranging about 2 (log scale). These data correlate with the promoter activity data, and suggest that AREG is controlled by H4 at transcriptional level.

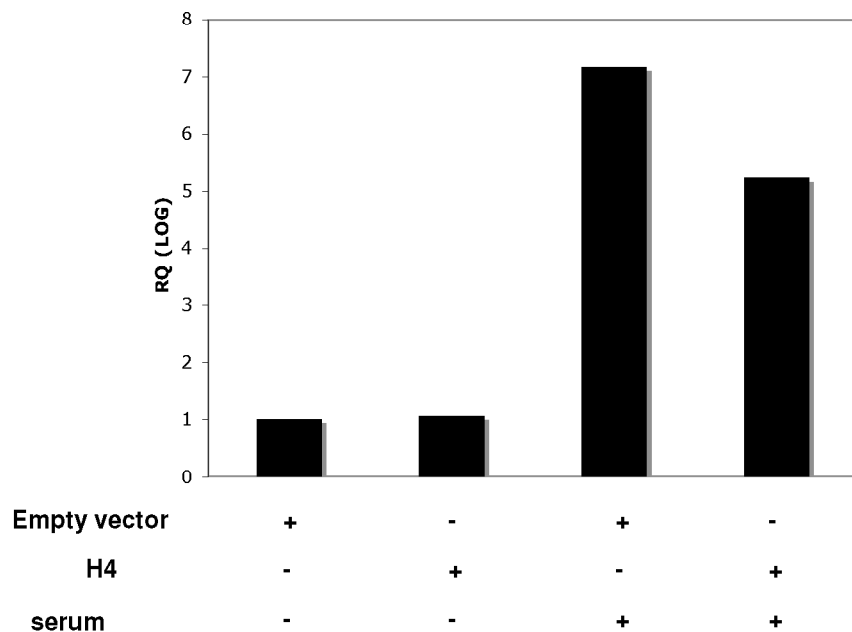


Figure 7 H4 reduces CREB1 target genes trascription

AREG expression in TPC1 cells transfected with pCMV and pCMV-H4. After 24 hrs of starvation by serum the cells were treated with serum for 2 hr and RNA was extract and analysed by qRT-PCR. The fold change indicates the relative value of the expression levels between pCMV without serum, pCMV with serum, pCMVH4 without serum, pCMVH4 with serum and pCMV without serum sample.

4.4 H4 reduces CREB1 binding to CRE element

In the attempt to identify the biochemical mechanisms underlying the negative effects of H4 in CREB1 target genes transcription, we performed experiment designed to investigate if H4 could affect this promoter function by preventing the interaction of Creb1 to the promoter. We performed EMSA assay analyzing the ability of nuclear extracts (2,5 ug) from Hela cells transfected with pCMV or pCMV-H4 to bind CRE radiolabelled oligonucleotide . As shown in figure 8 the CRE oligonucleotide specifically binds nuclear proteins, forming complexes with various electrophoretic mobilities (A and B arrows)(lane 1). The expression of H4(D10S170) reduced the binding nuclear extracts to CRE element (lane 2). Binding specificity was demonstrated by competition experiments showing loss of binding with the addition of a 200-fold molar excess of unlabelled CRE oligonucleotide (lane 3 and 4).

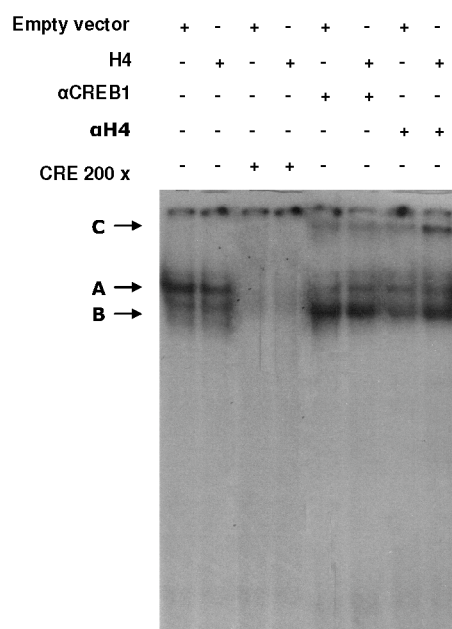


Figure 8 H4 binds the CRE element *in vitro*.

a) EMSA performed with a radiolabelled oligonucleotide containing the CRE element incubated with nuclear extracts (2,5 ug) from Hela cells transfected with pCMV or pCMV-H4 with or without the antibody indicated. Arrows indicate specific DNA/proteins complexes. To assess the specificity of the binding, nuclear extracts were incubated with a 200-fold excess of unlabelled oligonucleotide used as competitor.

In the attempt to determine the composition of these complexes, we have used specific antibody directed against the CREB or H4 proteins in a supershift analysis.

CRE oligonucleotide is able to form complexes with H4 and CREB. The antibody against CREB1 significantly reduced the band corresponding to complex A and

increased the band corresponding a faster-migrating complex B. Therefore, the complex DNA-CREB1 corresponds to the band A.

The antibody against H4 reduced the band corresponding to complex A and increased the band corresponding a slower-migrating complex C and a faster-migrating complex B. In pCMV-H4 nuclear extracts the presence of antibodies against H4 increased the binding of CREB to the CRE oligonucleotide. Taken together, these results indicated that H4 and CREB1 are in the same complex and that H4 reduces the binding of CREB1 to CRE element.

4.5 H4 requires Hdac activity to repress CREB1 target genes transcription

During the past 5 years, chromatin remodeling and histone modifications have emerged as the main mechanisms of the control of gene expression. The connection between DNA methylation and histone deacetylation in the silencing of genes has been established, and the mechanisms involve the participation of proteins belonging to the family of methyl-CpG binding domain proteins and HDACs. HDACs catalyze the removal of acetyl groups from core histones (Marks et al, 2001).

inducing local condensation of chromatin. Therefore, HDACs are generally considered repressors of transcription (Marks et al, 2001).

Tenbrock et al.(2006) presented evidence that CREM α regulates negatively gene transcription of CREB1 target genes and its binding to immune response gene promoters results in active recruitment of HDAC1, enhanced deacetylation of histones and transcriptional repression.

Therefore, we decided to investigate whether H4 could be mediating the repression of CREB1 target genes transcription by the recruitment of HDACs.

First, we analyzed HDAC activity in HeLa cells transfected with pCMV or pCMV-H4. Nuclear extracts were incubated with ^3H -labeled histones and the released [^3H] acetate was measured. H4 expression increased the HDAC activity in HeLa in a dose-dependent manner (the percentage of increase was 100% in HeLa cells, after the transfection of 8 μg of H4) (Figure 9).

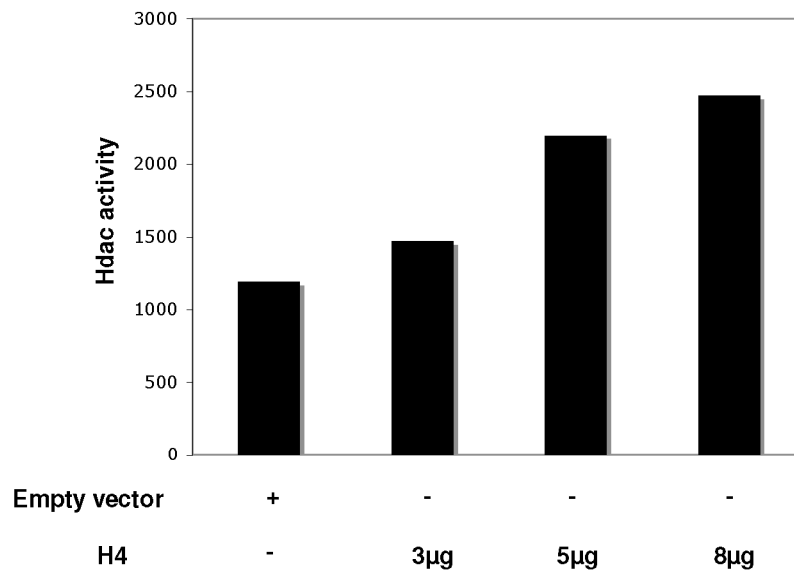


Figure 9 H4 stimulates HDAC activity.

HeLa cells were transfected with empty vector or with increasing amounts of H4 expression vector and nuclear extracts were assayed for HDAC activity after 48 h. Samples treated with sodium butyrate (NaB) were used as assay control. Values represent the average of three experiments +/- SD.

Then, we analyzed the effects of TSA, which specifically inhibits HDACs on the ability of H4 to increase the HDAC activity.

We analyzed HDAC activity in HeLa cells transfected with pCMV or pCMV-H4 (5µg) in presence or absence of TSA (300nM for 24 hrs). Nuclear extracts were incubated with ³H-labeled histones and the released [³H] acetate was measured. In absence of TSA, a significantly higher level of HDAC activity in pCMV-H4 extracts compared to pCMV extracts was observed, as previously observed. In presence of TSA, the HDAC activity was inhibited and the inhibition was stronger in the pCMV-H4 extracts with respect to the control (Figure 10). The data confirmed that H4 specifically increases Hdac activity.

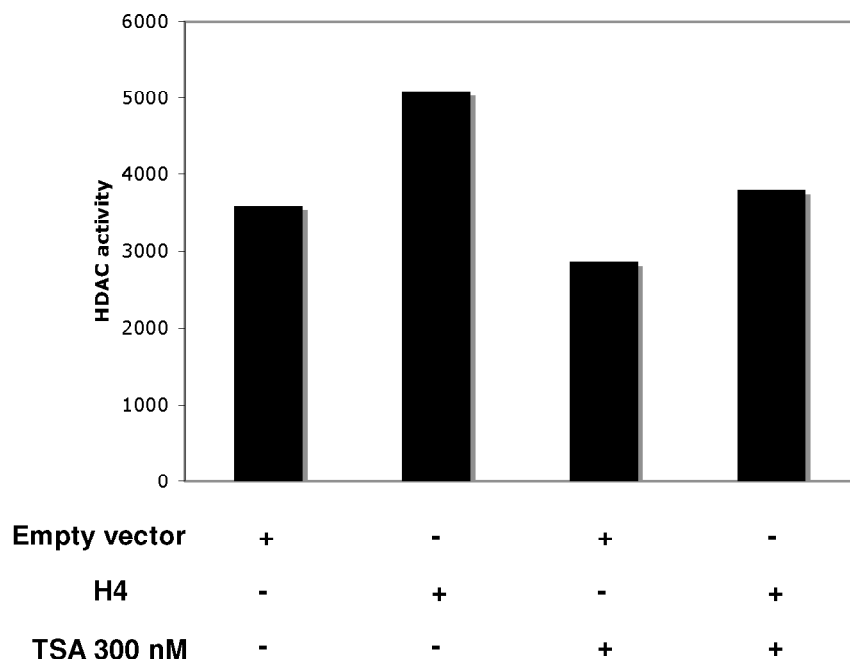


Figure 10 TSA inhibits the H4-mediated activation of the Hdac.

HeLa cells were transfected with empty vector or with H4 expression vector and nuclear extracts were assayed for HDAC activity after 24 h TSA treatment (300nM). Values represent the average of three experiments \pm SD

Finally, we, also, analyzed the effects of TSA in the H4-mediated repression of CREB1 target genes. To this end, I studied the repressor effect of H4 on the reporter Luc construct previously used in Hela cells. As shown in figure 11, the Luc reporter construct basal activity was increased by expressing of CREB1, the expression of CREB1 activated the reporter whereas the cotransfection of H4(D10S170) in hela cells reduced the activity of the CRE promoter to 50%, as previously observed. The treatment with TSA (300nM for 24 hrs) increase of 25% the activation of promoter in CREB1 trasfected cells and reduces the repressive effect of H4 . (Fig. 9). Taken together, these results suggest that HDAC activity is required for efficient H4 repression of the promoter CREB1 target genes. However, the inhibition of HDAC activity alone does not revert the repressive effect of H4, probably because the concentration of TSA used is not sufficient to completely inhibit the activity of HDAC1 or because the DNA methylation and histone acetylation interplay in gene silencing.

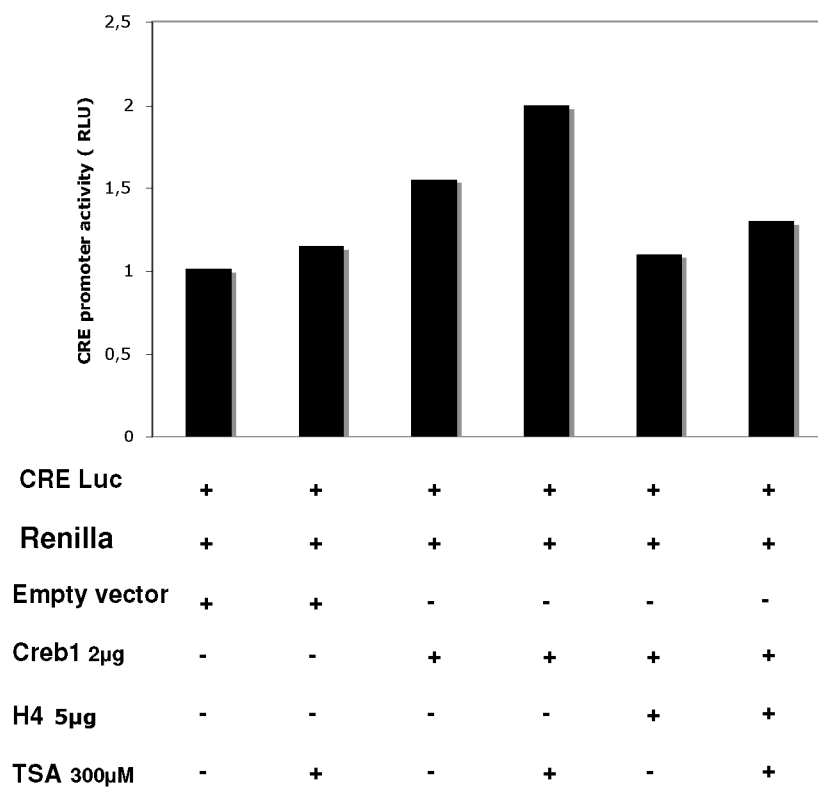


Figure 11 TSA inhibits the H4-mediated repression of the CRE promoter.

CRE promoter activity was analyzed in HeLa cells in the presence of plasmids pSPORT6CREB1 without or with pcDNA-H4. The cells were treated with TSA (300 nM;) or with ethanol for 24 h after transfection. Luciferase and Renilla activities were determined 24 h after treatment; Results represent the averages \pm standard deviations of at least two independent experiments performed in duplicate.

4.6 H4 associates with HDAC1

To get further insights into the model of H4-mediated repression, we decided to analyze the possibility that the requirement of HDAC activity could be mediated by interaction of H4 with the class I family of HDACs.

For this purpose, GST- H4 was tested for the ability to bind *in vitro* HDAC family proteins. Protein lysates from Hela cells were incubated with GSTH4 or GST beads for 2 hours, then the bound proteins were separated by SDSPage and the gels were analyzed by Western Blot using the antibody for HDAC1, 2 and 3.

As shown in fig 12A, no specific bands in the lane for GST and GST-H4 were detected when western blot was performed for α HDAC2, α HDAC3, the western blot for α HDAC1 showed a band in the lane for GST-H4 and no band in the lane for GST. The data confirmed a specific, direct physical interaction between H4(D10S170) and HDAC1, but not with other proteins of HDAC family.

Next, we confirmed this interaction *in vivo*. To this end, transient transfections of the Myc-HIS -tagged-H4 expression vector were performed in HELA cells . Protein lysates were immunoprecipitated with anti-H4 antibodies and immunoblotted with anti-Myc and anti-HDAC1 antibodies. As shown in Figure 12B, HDAC1 was coimmunoprecipitated by α H4 antibodies but not by IgG control antibodies. The data confirmed the association between H4 and the endogenous HDAC1 protein.

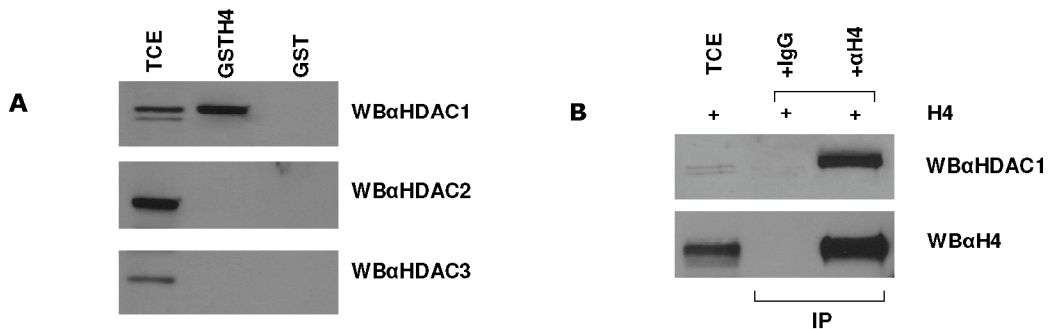


Figure12 H4 interacts with HDAC1.

A) *In vitro* interaction between H4 and CREB1.

GST pull-down assays were performed between total cell extracts (TCEs) from Hela cells and the GST or GST-H4 fusion protein. The bound complexes and TCEs were separated on SDS-PAGE and analysed by Western blotting with antibody for different proteins of HDAC family (α HDAC1, α HDAC2, α HDAC3 Upstate)

B) *In vivo* characterization of the H4/HDAC1 interaction.

Hela cells were transfected with pCMV/H4 vector. After 48 h, total cell extracts were prepared and proteins were immunoprecipitated with anti-H4. The immunocomplexes analysed by Western blotting using the reciprocal antibodies (antiH4 and antiHDAC1). The relative inputs are total cell extracts derived from Hela-transfected cells with the expression vector encoding H4. IgG indicates the negative control of immunoprecipitation using an unrelated antibody.

4.7 H4 interacts in vivo with the AREG promoter and recruits HDAC1 and reduces the binding of CREB1

Given that H4 has Proline rich domains which bind DNA, we asked whether the physical interaction between H4 and HDAC1 takes place on the human AREG promoter. Therefore, I first evaluated whether H4 protein binds the AREG promoter *in vivo* by ChIP assays. The ChIP assays was performed in H4-null papillary carcinoma cells (TPC1)

H4-null TPC1 cells were transfected with pCMV and pCMV-H4 and after 24 hrs of starvation, were treated with serum for 30 minutes, crosslinked, and immunoprecipitated with anti-H4, anti-CREB1 or anti-IgG antibodies. The precipitated DNA was subjected to PCR with specific primers for the endogenous CRE element Areg promoter region (-274/-267). Anti-H4 antibodies precipitated this AREG promoter region from TPC1 cells transfected with Myc-HIS-tagged-H4 protein (Figure 13). No precipitation was observed with anti-IgG precipitates, and when primers for the control promoter GAPDH were used (Figure 13, lower panel), indicating that the binding is specific for the AREG promoter. These results indicate that H4 protein binds the AREG promoter region *in vivo*.

To determine whether H4 occupies the Areg promoter together with HDAC1, the anti-H4 complexes were released, reimmunoprecipitated with anti-HDAC1, and then analysed by semiquantitative PCR (Re-ChIP). The results show that the antibodies against HDAC1 precipitate the Areg promoter in TPC1-H4 cells and not in the control after their release from anti-H4, indicating that H4 occupies this region with HDAC1 (Figure 13). The reciprocal experiment provided comparable results (Figure 13). Taken together, these results indicate that H4 binds the human Areg promoter *in vivo* and recruits HDAC1.

The binding of CREB1 was used as a positive control. As expected, anti-CREB1 precipitated this AREG region from TPC1 cells transfected with pCMV or with pCMVH4 (Figure 13) and the binding of CREB1 at the AREG promoter is reduced in TPC1-H4 cells.

Then I evaluated whether H4 can displace Creb1. In a combination of ChIP and Re-ChIP analyses, the anti-CREB1 complexes were released, reimmunoprecipitated with anti-H4. The results show that the antibodies against CREB1 precipitate the Areg promoter in TPC1 cells but not in TPC1-H4 after their release from anti-H4, indicating that H4 doesn't occupy this region with CREB1. Taken together, these results indicate that H4 *in vivo* displaces CREB1 from AREG promoter, in agreement to what observed *in vitro*.

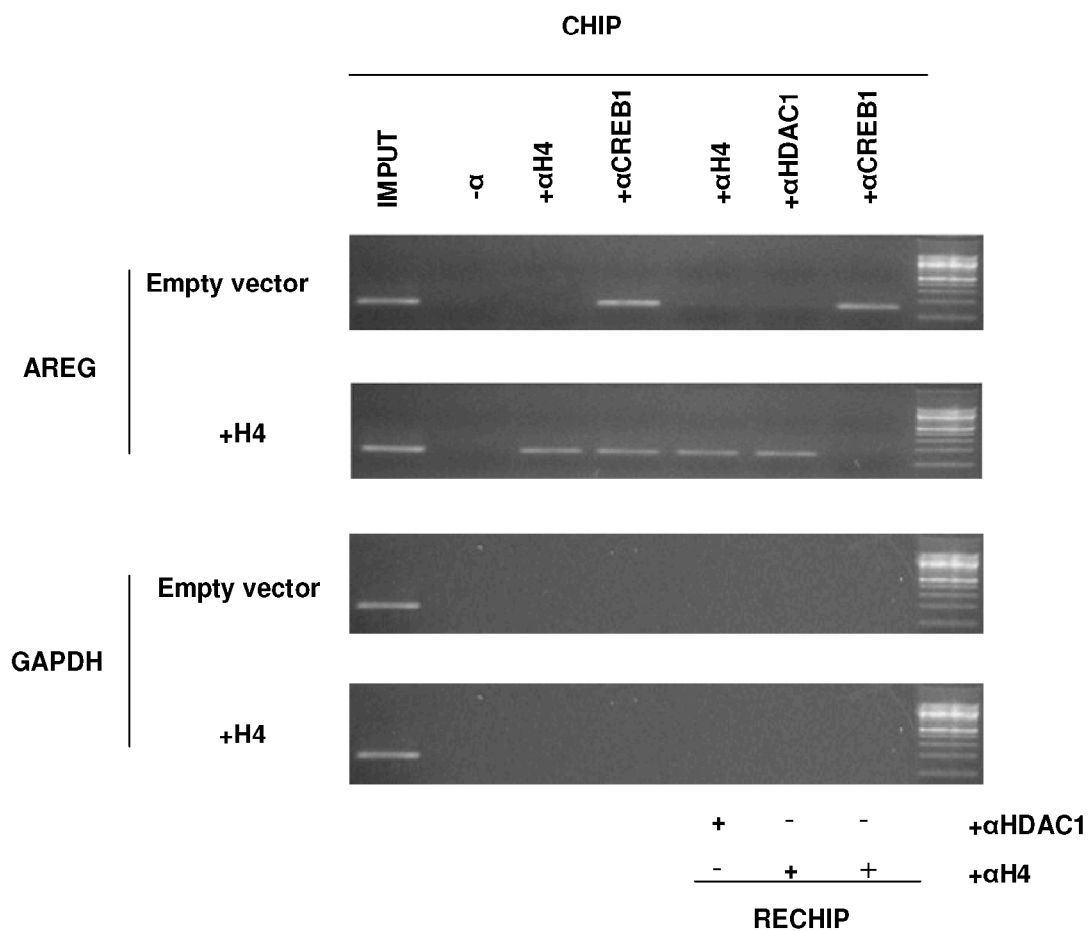


Figure13 H4 interacts with the endogenous AREG promoter and recruits HDAC1 and reduces the binding of CREB1

TPC1 cells were transfected with pCMV and pCMV-H4 and after 24 hrs of starvation by serum were treated with serum for 30 minutes, crosslinked, and immunoprecipitated with anti-H4, anti-CREB1. The precipitated DNA was subjected to PCR with specific primers that cover a region of human AREG promoter which contains the CRE element or primers for the GAPDH gene promoter as control. IgG were used as an immunoprecipitation control.

In Re-ChIP experiments, soluble chromatin from TPC1 cells transfected with pCMV or pCMVH4 was immunoprecipitated with anti-H4 or anti HDAC1 or anti CREB1 eluted, and reimmunoprecipitated with anti-HDAC1, or anti H4 respectively. The precipitated DNA was subjected to PCR.

4.8 H4 expression is correlated with AREG promoter deacetylation

These studies suggested that HDACs participate in the H4-mediated repression of CREB1 target genes. If H4 expression affects AREG gene expression levels, one would expect to observe changes in the histone acetylation status at its promoter. Therefore, our next goal was to check whether H4 expression correlated with histone deacetylation at the Areg promoter. To address this point, we analyzed the acetylation status of histones H3 at the Areg promoter by ChIP assays.

After the formaldehyde cross-linking of pCMV and pCMV-H4 cells, ChIP assays were performed with antibody against acetylated histones H3. The precipitated DNA was subjected to PCR with specific primers for the endogenous CRE element Areg promoter region (-274/-267). The analysis revealed that H4 expression is associated with a strong decrease in the levels of acetylated histones H3 at the AREG promoter. No precipitation was observed with anti-IgG precipitates, and when primers for the control promoter GAPDH were used (Figure 14, lower panel), indicating that the binding is specific for the *AREG* promoter.

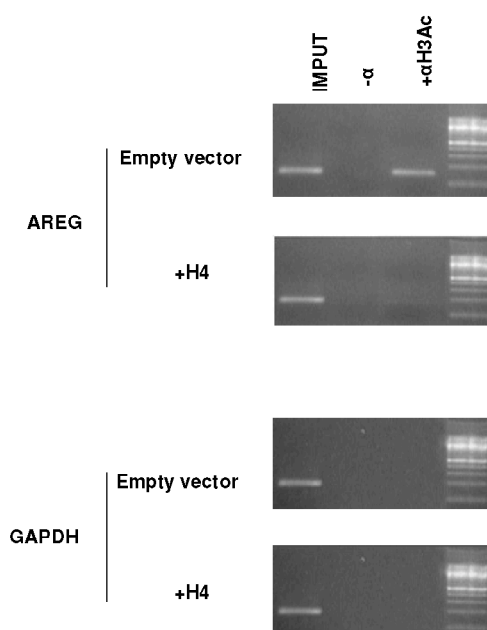


Figure 14 H4 expression is correlated with AREG promoter deacetylation

Soluble chromatin from TPC1 cells transfected with pCMV and pCMV-H4 was immunoprecipitated with anti-acetyl-histone H3 (α -Ac-H3). The DNAs were then amplified by semiquantitative PCR using primers that cover a region of human AREG promoter, which contains the CRE element. As an immunoprecipitation control, IgG was used. The panel shows also PCR amplification of the immunoprecipitated DNA using primers for the GAPDH gene promoter as control.

4.9 H4 Knock-out mice

To better characterize the biologic function of H4, we generated H4 Knockout mice. We used gene targeting techniques in embryonic stem (ES) cells to generate a null mutation at the murine H4 genomic locus. We deleted exon II, which contains coiled-coil domain and replaced it with a neomycin-resistance cassette (see Materials and Methods). Cell clones resistant to G418 have been isolated and screened for H4 homologous recombination. The positive clones were expanded and injected into blastocysts from the C57BL/6 mice strains. The resulting chimaeric blastocysts were transferred to uteri of foster mothers of the same strain. The chimaeric offspring was crossed with wild-type mice to obtain germ line transmission with the generation of mice heterozygous for H4 gene disruption. The heterozygous mice were then crossed with each other to generate homozygous mice. Chimeric males transmitted the mutated H4 allele through the germline, as demonstrated by PCR analysis of tail DNA (Figure 15) and by reverse transcriptase-polymerase chain reaction (RT-PCR) of H4^{+/+}, H4^{+/-}, and H4^{-/-} mice spleen (Figure 13).

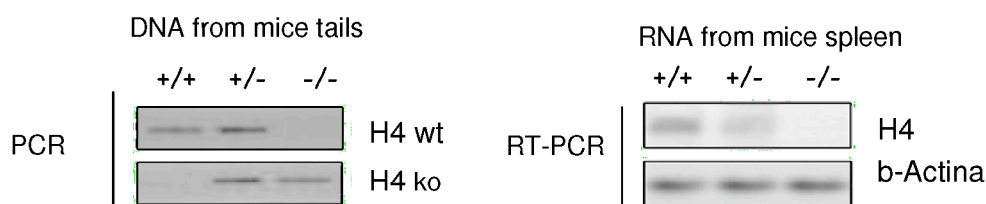


Figure 15. H4 Knockout Mice

A) PCR analysis of mouse genomic DNA from mouse tails.

B) RT-PCR analysis showing H4 gene expression in H4^{+/+}, H4^{+/-}, and H4^{-/-} mice spleen as indicated. Actin mRNA expression was used as a loading control.

4.10 H4 KO affects cell proliferation.

In order to evaluate the effect of H4 null mutation on cell growth, we analyzed the growth potential of MEFs (mouse embryonic fibroblast) derived from WT or KO embryos by growth-curve experiments. The cells were plated and cultured in complete medium, and counted every day for eleven consecutive days. As shown in Figure 16, the growth rate of H4^{-/-} MEFs was reduced compared with H4^{+/+} MEFs. In fact H4^{-/-} MEFs cultured in complete medium grew more slowly when compared to H4^{+/+} MEFs and did not reach the log phase.

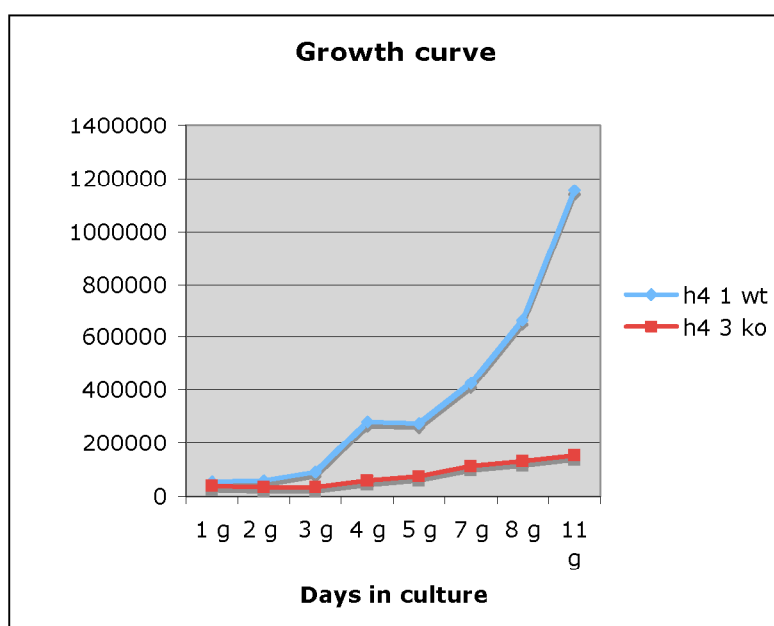


Fig. 16 Growth of H4 MEFs cells.

Growth curves of MEFs derived from WT or KO embryos. Cells were plated as described in "Materials and Methods" and counted daily for 11 days.

4.11 Cell cycle distribution

In order to individuate the cell cycle phase in which H4^{-/-} MEFs are blocked, we analyzed the cell cycle distribution of MEFs derived from WT or KO embryos cultured in complete medium. FACS analysis results showed an accumulation in the G2/M phases in H4^{-/-} MEFs compared to H4^{+/+} MEFs. (Fig17).

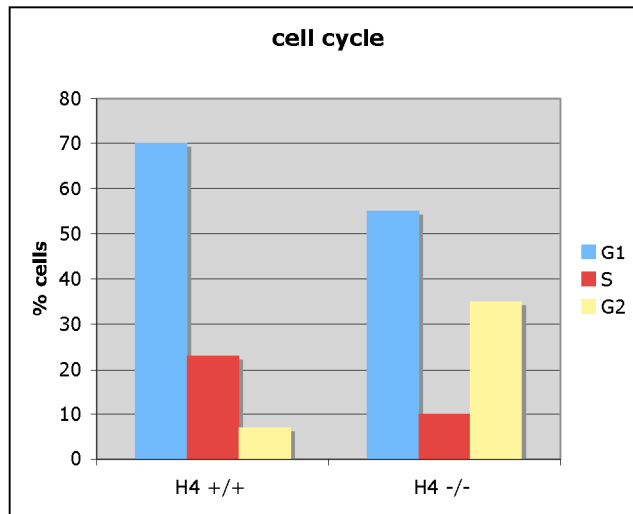


Figure 17 Cell cycle distribution of H4 MEFs.

MEFs derived from WT or KO embryos cultured in complete medium and analysed by FACS. Cell cycle analyses as described in "Materials and Methods."

4.12 Cyclin and CDK Expression pattern is altered in H4^{-/-} MEFs.

Since the progression through the cell cycle requires the coordinated activation of a family of protein kinases called CDKs (Reed 1994), we investigated the expression of cyclins and CDK proteins in MEFs derived from WT or KO embryos. Activation of each kinase is a highly regulated process beginning with: (a) the association of a CDK with a positive regulatory subunit called "cyclin"; (b) phosphorylation of a conserved threonine residue by a CDK-activating kinase; and/or (c) binding of inhibitory molecules, CDK inhibitors (Koff 1992, Matsushine 1994, Sherr 1995). G1 progression is controlled by sequential activation of cyclin D/CDK4–6 and cyclin E/CDK2 complexes, whereas entry into S-phase is mainly regulated by cyclin A/cdk2. Progression of cells through G2 into mitosis is controlled by sequential activation of cyclin A/Cdk2 and cyclin B/cdc2 complexes.

To analyze the expression of cyclins and CDK, the cells were synchronized by

starvation of serum and stimulated to reenter the cycle after 3 days, and then lysed at 6, 12, 18, 24, and 36 h. Subsequently, the expression of cyclins and CDK proteins were detected by Western blot. Cyclin D3 in H4+/+ MEFs was induced after 6 h of stimulation, (Figure 18) . Conversely, cyclin D3 was expressed in starved in H4-/- cells and increased at 6h. These data could indicate that H4 -/- MEFs enter the cell cycle earlier than H4 +/+ MEFs .The basal level of cyclin E protein was induced after 12 h of stimulation, with a peak at 18 and 36 h in H4 +/+ MEFs whereas increased at 6 h and decreased at 12 h in H4 -/- MEFs. CDK4 and cdc2 expression was not modified in H4 MEFs. Cyclin A was increased after 18 h of treatment in H4 +/+ MEF and decreased at 36h, whereas in H4 -/- MEFs its expression remained elevated since 6 to 36 hrs. The higher level of cyclin A in H4 -/- MEFs could be responsible of the accumulation of H4 -/- MEFs in G2/M phase.

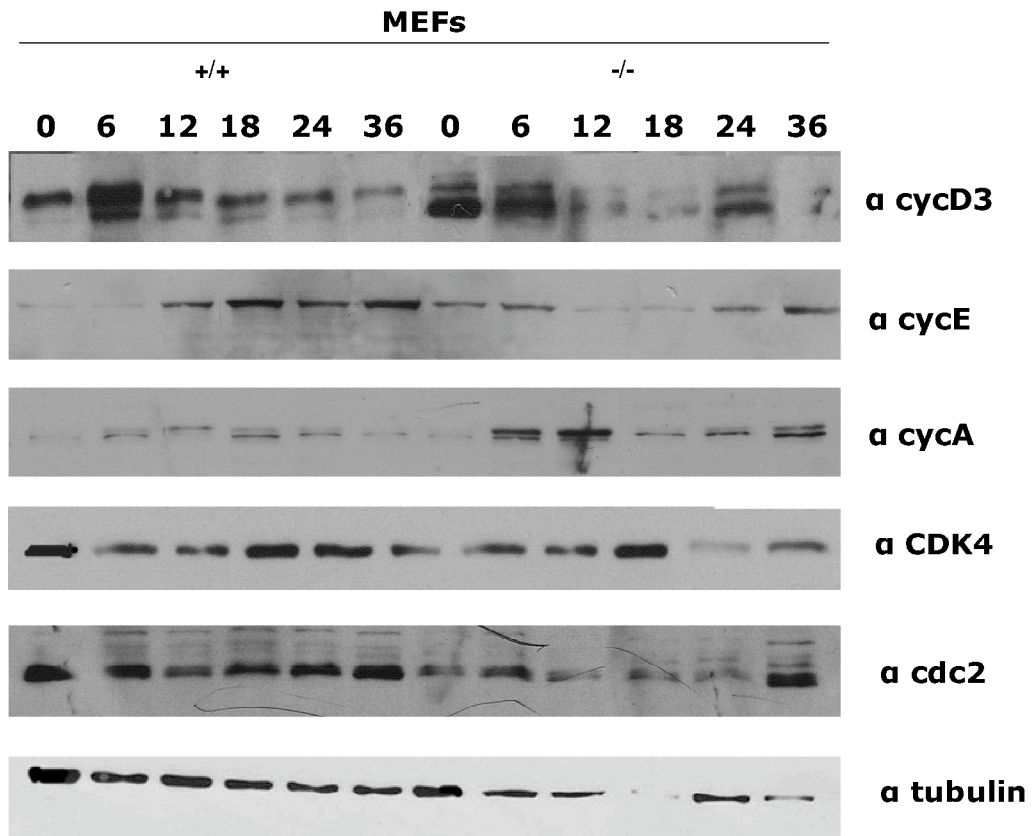


Figure 18 Expression of cell-cycle regulators in MEFs starved (0) and stimulated with serum for 6, 12, 18, 24, and 36 h. The expression of each cell-cycle regulator was determined by Western blot analyzes as described in "Materials and Methods."

4.13 H4 ^{-/-} MEFs induce apoptosis

In parallel with the cell cycle analysis, we investigated whether the block in G2/M phase induced cell death. We performed FACS analysis of MEFs derived from WT or KO embryos grown in complete medium or starved for 24 or 48h after annexin staining. As shown in figure 19 a consistent fraction of H4^{-/-} MEFs (30%) were Annexin positive, 8-fold more than H4^{+/+} MEFs. Then we confirmed the data at FACS analysis through expression of caspase 3, an interleukin 1b converting enzyme-like cysteine protease that is central to many apoptotic systems. Total cell extracts from WT or KO embryos grown in complete medium or starved for 48 h were blotted with an antibody raised against caspase 3. H4^{-/-} MEFs showed level higher of caspase 3 compared to the H4^{+/+} MEFs. The membrane was probed with antibodies raised versus tubulin to normalize.

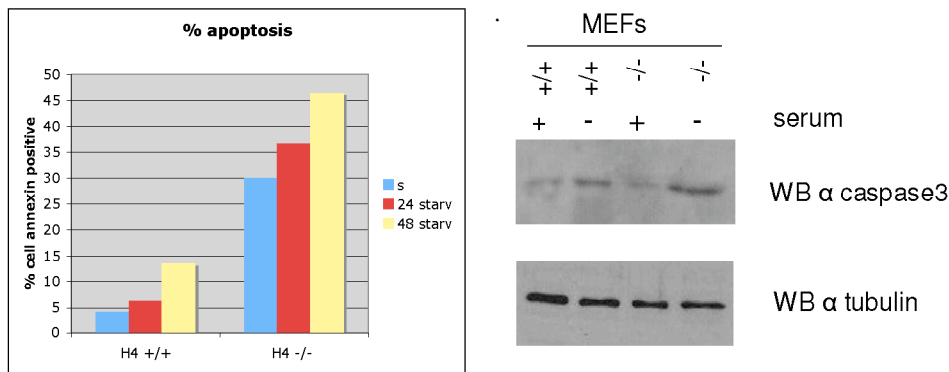


Figure 19 Apoptosis analysis in H4 knockout MEFs

A) Apoptosis analysis in WT or KO embryos grown in complete medium or starved for 24h or 48 h. Apoptosis was calculated as the percentage of cells positive at annexin V-FITC as described in Materials and Methods.

B) Western blot analysis of caspase3 expression in total cell extracts from WT or KO embryos grown in complete medium or starved for 48 h. Tubulin expression was used to normalize the amount of loaded proteins.

4.14 Activation of CREB1 in H4 ^{-/-} MEFs

Taken together the data on the proliferation rate, block in G2/M and apoptosis performed on the H4 MEFs indicate that H4 is implicated in the control of cell cycle and its role is probably related to its capacity to inhibit the transcription of gene target of CREB1. In fact, the literature is rich of studies showing that CREB1 inhibits proliferation in fibroblasts.(Porcellini 2003) Moreover, its constitutive activation induces meiotic arrest at the G2/M transition in

mammalian oocytes (Conti 2002). Mehlmann(2002) says that this block is dependent on the presence of an active Gs protein. In fact, the inhibition of Gs by injection of a Gs α inhibitory antibody in the *Pde3a*-deficient oocytes induces a prompt reentry into the cell cycle. Similarly, the inhibition of steps downstream of cAMP, such as PKA catalytic activity, restores meiotic maturation in these oocytes (Masciarelli et al. 2004). We analysed the level of phosphorylation of CREB1 in MEFs. Total cell extracts from WT or KO embryos grown in complete medium were blotted with an antibodies raised versus PCREB ser 133. The membrane was probed with antibody raised versus CREB1 to normalize. As shown in figure 20 the H4^{-/-} MEFs have level higher of PCREB than the H4^{+/+} MEFs (figure 20). Therefore, the H4^{-/-} MEFs could show G2/M block and inhibition of proliferation for constitutive activation of CREB1 trascription in absence of H4. These data in vivo are in agreement to what observed in vitro. H4, in fact, represses the activity of CREB1 reducing its phosphorylation .

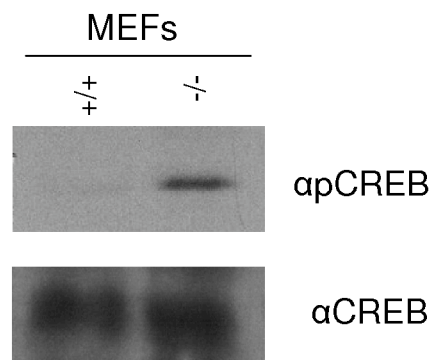


Figure 20 Expression of PCREB1/CREB in MEFs

Western blot analysis of PCREB ser 133 expression in total cell extracts from WT or KO embryos grown in complete medium. CREB expression was used to normalize the amount of loaded proteins.

5. Conclusions

Most human thyroid papillary carcinomas are characterized by rearrangements of the RET protooncogene with a number of heterologous genes, which generate the RET/papillary thyroid carcinoma (PTC) oncogenes.

RET/PTC rearrangements are considered early events in the tumorigenesis process because they are frequently found in clinically silent small PTCs (Viglietto *et al.*, 1995). The gene H4 is one of heterologous genes that most frequently is fused to the intracellular kinase-encoding domain of RET in papillary thyroid tumours. This rearrangement generates the RET/PTC1 oncogene that display constitutive Kinase activity. The 90% papillary thyroid tumours, that harbours the RET/PTC1 rearrangement, has lost the expression of the normal unrearranged H4(D10S170) allele. The loss of the normal allele of this gene might result in growth advantage in tumour progression.

Here, we conducted a study for functional characterization of H4 gene. Our results demonstrated that H4 is responsible for transcriptional repression of CREB1 target genes by a chromatin-dependent mechanism. We demonstrated that H4 requires histone deacetylase (HDAC) activity to repress the transcription and the treatment with trichostatin A (TSA), an HDAC inhibitor, is useful to block the repressor effect of H4. Moreover, H4 associates with histone deacetylase 1 (HDAC1) and recruits HDAC1 on CRE site of CREB1 target genes, in particular AREG (amphiregulin) promoter gene.

The H4-mediated recruitment of HDAC1 increased deacetylation of histones H3 and contributes to close chromatin structure and to repress promoter activity.

The involvement of H4 in the transcriptional regulation of CREB1 target genes is important in thyroid cells since thyroid cells are dependent on TSH for growth and differentiation. TSH activates its specific receptor in thyroid cells and induces cAMP pathway. In fact, TSH binds a seven-loop transmembrane receptor and activates a Gs protein which induces adenylyl cyclase. cAMP binds the regulatory subunits of PKA which releases the free catalytic subunit that phosphorylates CREB in SER133. CREB binds to target promoter and recruits the transcriptional apparatus.

So the loss of the normal allele of H4 in the 90% papillary thyroid tumours, that harbours the RET/PTC1, might result in growth advantage in tumour progression since the CREB pathway is not negatively regulated.

Taken together, the data presented here, contain general implication that can be extended also to other cell types and other tumor types, since the c-AMP responsive factor CREB have been shown to function in a broad array of biologic processes such as glucose metabolism and in complex neuronal functions like learning and memory (Lonze and Ginty 2002, Mayr and Montminy 2001) and in a broad array of tumorigenic processes such as cell survival and cell proliferation through binding of this protein to the promoter target and recruitment of transcriptional apparatus.

To efforce this hypothesis, the H4(D10S170) gene product is a ubiquitously

expressed protein and this could be explained by role of H4 in the regulation of CREB1 transcription.

Moreover, the data presented here, demonstrate that H4 inhibits the transcription of AREG, that has an antiapoptotic function in non small cell lung cancer cell lines, so H4 could exercise its proapoptotic function also reducing the expression of AREG.

Our results, therefore, strongly suggest that H4 could have a tumour suppressor role in thyroid carcinogenesis, by inhibiting the expression of proteins induced by CREB1.

6. ACKNOWLEDGEMENTS

I would like to acknowledge Prof. Giancarlo Vecchio who directed this Doctorate Program.

I wish to thank Prof. Alfredo Fusco, who supervised my work. His extraordinary knowledge of oncology, his great enthusiasm and his kindness are really unique. It has been a pleasure for me to work in his laboratory at DBPCM.

I would like to thank all the members of my laboratory for the support, the friendship and the enlightening scientific discussions.

I wish also to thank all the friends and colleagues at the Dipartimento di Biologia e Patologia Cellulare e Molecolare and at the Ceinge which made these years a great experience.

I am particularly indebted to Prof Carlo Croce for his kind hospitality during my visit at the Comprehensive Cancer Center – Ohio State University, Columbus, Ohio, USA. I profited a lot from discussion with the members of his group.

7.REFERENCES

- Andeniran A, Zhu Z, Gandhi M, Steward DL, Fidler JP, Giordano TJ, Biddinger PW, Nikiforov YE: Correlation between genetic alterations and microscopic features, clinical manifestations and prognostic characteristics of thyroid papillary carcinomas. *Am J Surg Pathol* 2006; 30:216–222.
- Asklen LA, LiVolsi VA: Prognostic significance of histological grading compared with sub classification of papillary thyroid carcinoma. *Cancer* 2000; 88:1902–1908.
- Bakkenist CJ, Kastan MB: DNA damage activates ATM through intermolecular autophosphorylation and dimer dissociation. *Nature*. 2003 Jan 30;421(6922):499-506.
- Bongarzone I, Vigneri P, Mariani L, Collini P, Pilotti S, Pierotti MA: RET/NTRK1 rearrangements in thyroid gland tumors of the papillary carcinoma family: Correlation with clinic pathologic features. *Clin Cancer Res* 1998;4:223–228.
- Capella G, Matias-Guiu X, Ampadia X, de Leiva A, Perucho M, Prat J : Ras oncogene mutations in thyroid tumors: Polymerase chain reaction restriction-fragment-length polymorphism analysis from paraffin embedded tissue. *Diagn Mol Pathol* 1996;5:45–52.
- Carcangiu, ML, Zampi, G. & Rosai, J. Poorly differentiated ('insular') thyroid carcinoma. A reinterpretation of Langhans' 'wuchernde Struma'. *Am J Surg Pathol* 1984;8, 655–668.
- Carlezon WA Jr, Duman RS, Nestler EJ: The many faces of CREB. *Trends Neurosci*. 2005 Aug; 28(8):436-45.
- Celetti A, Cerrato A, Merolla F, Vitagliano D, Vecchio G, Grieco M: H4(D10S170), a gene frequently rearranged with RET in papillary thyroid carcinomas: functional characterization. *Oncogene*. 2004 Jan 8;23(1):109-21.
- Chawla S, Bading H: CREB/CBP and SRE-interacting transcriptional regulators are fast on-off switches: duration of calcium transients specifies the magnitude of transcriptional responses. *J Neurochem*. 2001 Nov; 79(4):849-58.
- Ciampi R, Knauf JA, Kerler R, Gandhi M, Zhu Z, Nikiforova MN, Rabes HM, Fagin JA, Nikiforov YE: Oncogenic AKAP9-BRAF fusion is a novel mechanism of MAPK pathway activation in thyroid cancer. *J Clin Invest* 2005;115:94–101.

Ciampi R, Nikiforov YE: Alterations in BRAF in thyroid tumors. *Endocrinol Pathol* 2005;16:163–171.

Cohen Y, Xing M, Mambo E, Guo Z, Wu G, Trink B, Beller U, Westra WH, Ladenson PW, Sidransky D: BRAF mutation in papillary thyroid carcinoma. *J Nat'l Cancer Inst* 2003;95:625–627.

Conti M, Andersen CB, Richard F, Mehats C, Chun SY, Horner K, Jin C, Tsafirri A: Role of cyclic nucleotide signaling in oocyte maturation. *Mol Cell Endocrinol*. 2002 Feb 22;187(1-2):153-9.

Davies H, Bignell GR, Cox C, Stephens P, Edkins S, Clegg S, Teague J, Woffendin H, Garnett MJ, Bottomley W, Davis N, Dicks E, Ewing R, Floyd Y, Gray K, Hall S, Hawes R, Hughes J, Kosmidou V, Menzies A, Mould C, Parker A, Stevens C, Watt S, Hooper S, Wilson R, Jayatilake H, Gusterson BA, Cooper C, Shipley J, Hargrave D, Pritchard-Jones K, Maitland N, Chenevix-Trench G, Riggins GJ, Bigner DD, Palmieri G, Cossu A, Flanagan A, Nicholson A, Ho JW, Leung SY, Yuen ST, Weber BL, Seigler HF, Darrow TL, Paterson H, Marais R, Marshall CJ, Wooster R, Stratton MR, Futreal PA : Mutations of the BRAF gene in human cancer. *Nature (London)* 2002;417:949–954.

Davies L, Welch HG: Increasing incidence of thyroid cancer in the United States, 1973–2002. *JAMA* 2006;295:2164–2167.

De Felice M, Di Lauro R. Thyroid Development and Its Disorders: Genetics and Molecular Mechanisms. *Endocrine Reviews* 2004;25:722–46.

De Lellis L, Curia MC, Catalano T, De Toffol S, Bassi C, Mareni C, Bertario L, Battista P, Mariani-Costantini R, Radice P, Cama A. Combined use of MLPA and nonfluorescent multiplex PCR analysis by high performance liquid chromatography for the detection of genomic rearrangements. *Hum Mutat*. 2006 Oct;27(10):1047-56.

Di Christofaro J, Marcy M, Vasko V, Sebag F, Fakhry N, Wynford-Thomas D, De Micco C: Molecular genetic study comparing follicular variant versus classic papillary thyroid carcinomas: Association of N-ras mutation in codon 61 with follicular variant. *Hum Pathol* 2006;37:824–830.

Dolmetsch RE, Pajvani U, Fife K, Spotts JM, Greenberg ME: Signaling to the nucleus by an L-type calcium channel-calmodulin complex through the MAP kinase pathway. *Science*. 2001 Oct 12; 294(5541): 333-9.

Donghi R, Longoni A, Pilotti S, Michieli P, Della Porta G, and Pierotti MA: Gene p53 mutations are restricted to poorly differentiated and undifferentiated carcinomas of the thyroid gland. *J Clin Invest* 1993;91:1753-60.

Eng C. Multiple endocrine neoplasia type 2 and the practice of molecular medicine.

Rev Endocr Metab Disord. 2000 Nov;1(4):283-90.

Fagin JA, Matsuo K, Karmakar A, Chen DL, Tang SH, Koeffler HP. High prevalence of mutations of p53 gene in poorly differentiated human thyroid carcinomas. *J Clin Invest* 1993;91:179-84.

Fink A, Tomlinson G, Freeman JL, Rosen IB, Asa SL: Occult micropapillary carcinoma associated with benign follicular thyroid disease and unrelated thyroid neoplasms. *Mod Pathol* 1996;9:816–820.

Fischer AH, Bond JA, Taysavang P, Battles OE, Wynford-Thomas D : Papillary thyroid carcinoma oncogene (RET/PTC) alters the nuclear envelope and chromatin structure. *Am J Pathol* 1998;153:1443–1450.

Fontaine J. Multistep migration of calcitonine cell precursors during ontogeny of the mouse pharynx. *Gen Comp Endocrinol* 1979;37:81–92.

Fukushima T, Suzuki S, Mashiko M, Ohtake T, Endo Y, Takebayashi Y, Sekikawa K, Hagiwara K, Takenoshita S: BRAF mutations in papillary carcinomas of the thyroid. *Oncogene* 2003;22:6455–6457.

Fusco A, Grieco M, Santoro M, Berlingieri MT, Pilotti S, Pierotti MA, Della Porta G, Vecchio G: A new oncogene in human papillary carcinomas and their lymph nodal metastases. *Nature* 1987;328:170–172.

Gasbarri A, Sciacchitano S, Marasco A, Papotti M, Di Napoli A, Marzullo A, Yushkov P, Ruco L, Bartolazzi A. Detection and molecular characterisation of thyroid cancer precursor lesions in a specific subset of Hashimoto's thyroiditis. *Br J Cancer.* 2004 Sep 13;91(6):1096-104.

Gavin AC, Bosche M, Krause R, Grandi P, Marzioch M, Bauer A, Schultz J, Rick JM, Michon AM, Cruciat CM, Remor M, Höfert C, Schelder M, Brajenovic M, Ruffner H, Merino A, Klein K, Hudak M, Dickson D, Rudi T, Gnau V, Bauch A, Bastuck S, Huhse B, Leutwein C, Heurtier MA, Copley RR, Edelmann A, Querfurth E, Rybin V, Drewes G, Raida M, Bouwmeester T, Bork P, Seraphin B, Kuster B, Neubauer G, Superti-Furga G: Functional organization of the yeast proteome by systematic analysis of protein complexes. *Nature.* 2002 Jan 10; 415(6868):141-147.

Gorbman A: Comparative anatomy and physiology. In: Ingbar SI, Braverman LE, eds. The thyroid. Philadelphia: JB Lippincott Company;1986:p. 43–52.

Greco A, Roccato E, Pierotti MT: TRK oncogenes in papillary thyroid carcinoma. *Cancer Treat Res.* 2004;122:207–219.

Grieco M, Cerrato A, Santoro M, Fusco A, Melillo RM, Vecchio G: Cloning and characterization of H4 (D10S170), a gene involved in RET rearrangements in vivo. *Oncogene.* 1994 Sep; 9(9):2531–5.

Grieco M, Santoro M, Berlingieri MT, Melillo RM, Donghi R, Bongarzone I, Pierotti MA, Della Porta G, Fusco A, Vecchio G: PTC is a novel rearranged form of the ret protooncogene and is frequently detected in vivo in human papillary thyroid carcinomas. *Cell* 1990;60:557.i–563.i.

Harach HR, Escalante DA, Day ES. Thyroid cancer and thyroiditis in Salta, Argentina: a 40-yr study in relation to iodine prophylaxis. *Endocr Pathol.* 2002 Fall;13(3):175–81.

Ho Y, Gruhler A, Heilbut A, Bader GD, Moore L, Adams SL, Millar A, Taylor P, Bennett K, Boutilier K, Yang L, Wolting C, Donaldson I, Schandorff S, Shewnarane J, Vo M, Taggart J, Goudreault M, Muskat B, Alfarano C, Dewar D, Lin Z, Michalickova K, Willems AR, Sassi H, Nielsen PA, Rasmussen KJ, Andersen JR, Johansen LE, Hansen LH, Jespersen H, Podtelejnikov A, Nielsen E, Crawford J, Poulsen V, Sørensen BD, Matthiesen J, Hendrickson RC, Gleeson F, Pawson T, Moran MF, Durocher D, Mann M, Hogue CW, Figeys D, Tyers M: Systematic identification of protein complexes in *Saccharomyces cerevisiae* by mass spectrometry. *Nature.* 2002 Jan 10; 415(6868):180–183.

Hunt JL, Tometsko M, LiVolsi VA, Swalsky P, Finkelstein SD, Barnes EL: Molecular evidence of anaplastic transformation in coexisting well-differentiated and anaplastic carcinomas of the thyroid. *Am J Surg Pathol* 2003;27, 1559–1564.

Hurbin A, Dubrez L, Coll JL, Favrot MC: Inhibition of apoptosis by amphiregulin via an insulin-like growth factor-1 receptor-dependent pathway in non-small cell lung cancer cell lines. *J Biol Chem.* 2002 Dec 20;277(51):49127–33. Epub 2002 Sep 27.

Ito T, Seyama T, Mizuno T, Tsuyama N, Hayashi T, Hayashi Y, Dohi K, Nakamura N, Akiyama M: Unique association of p53 mutations with undifferentiated but not differentiated carcinomas of the thyroid gland. *Cancer Res* 1992;52:1369–71.

Jiang SM: The RET proto-oncogene in human cancers. *Oncogene*. 2000 Nov 20;19(49):5590-7

Johannessen M, Delghandi MP, Seternes OM, Johansen B, Moens U: Synergistic activation of CREB-mediated transcription by forskolin and phorbol ester requires PKC and depends on the glutamine-rich Q2 transactivation domain. *Cell Signal*. 2004 Oct; 16(10):1187-99.

Josselyn SA, Nguyen PV: CREB, synapses and memory disorders: past progress and future challenges. *Curr Drug Targets CNS Neurol Disord*. 2005 Oct; 4(5):481-97

Kastan MB, Lim DS: The many substrates and functions of ATM. *Nat Rev Mol Cell Biol*. 2000 Dec;1(3):179-86.

Kebebew, E, Greenspan, FS, Clark, OH, Woeber, KA & McMillan, A. Anaplastic thyroid carcinoma. Treatment outcome and prognostic factors. *Cancer* 2005;103, 1330–1335.

Kimura ET, Nikiforova MN, Zhu Z, Knauf JA, Nikiforov YE, Fagin JA: High prevalence of BRAF mutations in thyroid cancer. Genetic influence for constitutive activation of the RET/PTC-RAS-BRAF signaling pathway in papillary thyroid carcinoma. *Cancer Res* 2003;63: 1454–1457.

Kimura T, Van Keymeulen A, Golstein J, Fusco A, Dumont JE, Roger PP: Regulation of thyroid cell proliferation by TSH and other factors: a critical evaluation of in vitro models. 2001; *Endocr. Rev* 22, 631-656.

Knauf JA, MA X, Smith EP, Zhang L, Mitsutake N, Liao XH, Refetoff S, Nikiforov YE, Fagin JA : Targeted expression of BRAF600E in thyroid cells of transgenic mice results in papillary thyroid carcinoma that undergo differentiation. *Cancer Res* 2005; 65:4230–4245.

Koff A, Giordano A, Desai D, Yamashita K, Harper JW, Elledge S, Nishimoto T, Morgan D.O, Franza BR, Roberts JM: Formation and activation of a cyclin E-cdk2 complex during the G1 phase of the human cell cycle. *Science (Wash. DC)*, 257: 1689-1694, 1992.

Kondo T, Ezzat S, Asa SL. Pathogenetic mechanisms in thyroid follicular-cell neoplasia. *Nat Rev Cancer* 2006;6:292–306.

Krishan A: Rapid flow cytofluorometric analysis of mammalian cell cycle by propidium iodide staining. *J. Cell Biol.*, 66: 188-193, 1975.

Kroll TG, Sarraf P, Pecciarini L, Chen CJ, Mueller E, Spiegelman BM, and Fletcher JA: PAX-8-PPARgamma1 fusion oncogene in human thyroid carcinoma. *Science* 2000;289:1357–60.

Kulkarni S, Heath C, Parker S, Chase A, Iqbal S, Pocock CF, Kaeda J, Cwynarski K, Goldman JM, Cross NC: Fusion of H4/D10S170 to the platelet-derived growth factor receptor beta in BCR-ABL-negative myeloproliferative disorders with a t(5;10)(q33;q21). *Cancer Res.* 2000 Jul 1;60(13):3592-8.

Le Douarin N, Fontaine J, LeLievre C: New studies on the neural crest origin of the avian ultimobranchial glandular cells. Interspecific combinations and cytochemical characterization of Ccells based on the uptake of biogenic amine precursors. *Histochemie* 1974;38:297–305.

Lee JH, Paull TT: Direct activation of the ATM protein kinase by the Mre11/Rad50/Nbs1 complex. *Science.* 2004 Apr 2;304(5667):93-6.

Leskov KS, Criswell T, Antonio S, Li J, Yang CR, Kinsella TJ, Boothman DA. When X-ray-inducible proteins meet DNA double strand break repair. *Semin Radiat Oncol.* 2001 Oct;11(4):352-72.

Lin HY, Harris TL, Flannery MS, Aruffo A, Kaji EH, Gorn A, Kolakowski LF Jr, Lodish HF, Goldring SR: Expression cloning of an adenylate cyclase-coupled calcitonin receptor. *Science* 1991;254:1022–4.

LiVolsi VA, Asa SL: The demise of follicular carcinoma of the thyroid gland. *Thyroid* 1994;4, 233–236.

LiVolsi VA, Albores-Saavedra J, Asa SL, et al: Papillare carcinoma. In: DeLellis RA, Lloyd RV, Heitz PU, Eng C. editors. *Pathology and Genetics of Tumours of Endocrine Organs.* Lyon: IARC Press. 2004;57–66.

Lloyd RV, Erickson LA, Casey MB, Lam KY, Lohse CM, Asa SL, Chan JK, DeLellis RA, Harach HR, Kakudo K, LiVolsi VA, Rosai J, Sebo TJ, Sobrinho-Simoes M, Wenig BM, Lae ME. Observer variation in the diagnosis of follicular variant of papillary thyroid carcinoma. *Am J Surg Pathol* 2004;28:1336–1340.

Lonze BE, Ginty DD. Function and regulation of CREB family transcription factors in the nervous system. *Neuron.* 2002 Aug 15;35(4):605-23.

Marks P, Rifkind RA, Richon VM, Breslow R, Miller T, Kelly WK
Histone deacetylases and cancer: causes and therapies. *Nat Rev Cancer.* 2001 Dec;1(3):194-202.

Masciarelli S, Horner K, Liu C, Park SH, Hinckley M, Hockman S, Nedachi T, Jin C, Conti M, Manganiello V: Cyclic nucleotide phosphodiesterase 3A-deficient mice as a model of female infertility. *J Clin Invest.* 2004 Jul;114(2):196-205.

Matsushime H, Quelle DE, Shurtleff SA, Shibuya M, Sherr CJ, Kato JY:D-type cyclin-dependent kinase activity in mammalian cells. *Mol. Cell Biol.*, 3: 2066-2076, 1994.

Mayr B, Montminy M: Transcriptional regulation by the phosphorylation-dependent factor CREB. *Nat Rev Mol Cell Biol.* 2001 Aug; 2(8): 599-609.

Mauchamp J, Mirrione A, Alquier C, Andre` F. Follicle-like structure and polarized monolayer: role of the extracellular matrix on thyroid cell organization in primary culture. *Biol Cell* 1998;90:369–80.

McCurrach ME, Lowe SW: Methods for studying pro- and antiapoptotic genes in nonimmortal cells. *Methods Cell Biol.* 2001;66:197-227.

Mehlmann LM, Jones TL, Jaffe LA: Meiotic arrest in the mouse follicle maintained by a Gs protein in the oocyte. *Science.* 2002 Aug 23; 297 (5585):1343-5.

Merolla F, Pentimalli F, Pacelli R, Vecchio G, Fusco A, Grieco M, Celetti A: Involvement of H4(D10S170) protein in ATM-dependent response to DNA damage. *Oncogene.* 2007 Sep 13;26(42):6167-75. Epub 2007 Apr 9.

Namba H, Rubin SA, Fagin JA: Point mutations of ras oncogene are an early event in thyroid carcinogenesis. *Mol Endocrinol* 1990;4:1474–1479.

Nicholson GC, Moseley JM, Sexton PM, Mendelsohn FA, Martin TJ: Abundant calcitonin receptors in isolated rat osteoclasts. Biochemical and autoradiographic characterization. *J Clin Invest* 1986;78:355–60.

Nikiforov Y, Gnepp DR: Pediatric thyroid cancer following the Chernobyl disaster. Pathomorphologic study of 84 cases (1991–1992) from the Republic of Belarus. *Cancer* 1994;74:748–766.

Nikiforov Y: RET/PTC rearrangement in thyroid tumors. *Endoc Pathol* 2002;13:3–16.

Nikiforov YE, Erickson LA, Nikiforova MN, Caudill CM, Lloyd RV: Solid variant of papillary thyroid carcinoma: Incidence, clinical-pathological characteristics, molecular analysis and biological behavior. *Am J Surg Pathol* 2001;25:1478–1484.

Nikiforova MN, Kimura ET, Gandhi M, Biddinger PW, Knauf JA, Basolo F, Zhu Z, Giannini R, Salvatore G, Fusco A, Santoro M, Fagin JA, Nikiforov YE: BRAF mutations in thyroid tumors are restricted to papillary carcinomas and anaplastic or poorly differentiated carcinomas arising from papillary carcinomas. *J Endocrinol Metab* 2003;88:5399–5404.

Nikiforova MN, Stringer JR, Blough R, Medvedovic M, Fagin JA, Nikiforov YE : Proximity of Chromosomal loci that participate in radiation-induced rearrangements in human cells. *Science* 2000; 290:138–141.

Pierotti MA, Greco A: Oncogenic rearrangements of the NTRK1/NGF receptor. *Cancer Lett* 2006;232:90–8.

Porcellini A, Messina S, De Gregorio G, Feliciello A, Carlucci A, Barone M, Picascia A, De Blasi A, Avvedimento EV. The expression of the thyroid-stimulating hormone (TSH) receptor and the cAMP-dependent protein kinase RII beta regulatory subunit confers TSH-cAMP-dependent growth to mouse fibroblasts. *J Biol Chem*. 2003 Oct 17;278(42):40621-30. Epub 2003 Aug 5.

Puxeddu E, Zhao G, Stringer JR, Medvedovic M, Moretti S, Fagin JA: Characterization of novel non-clonal intrachromosomal rearrangements between the H4 and PTEN genes (H4/PTEN) in human thyroid cell lines and papillary thyroid cancer specimens. *Mutat Res*. 2005 Feb 15;570(1):17-32.

Quiros RM, Ding HG, Gattuso P, Prinz RA, Xu X : Evidence that one subset of anaplastic thyroid carcinomas are derived from papillary carcinomas due to BRAF and p53 mutations. *Cancer* 2005;103: 2261–2268.

Rabes HM, Demidchik EP, Siderow JD, Lengfelder E, Beimfohr C, Hoelzel D, Klugbauer S: Pattern of radiation induced RET and NTRK rearrangements in 191 post-Chernobyl papillary thyroid carcinomas: Biological, phenotypic and clinical implications. *Clin Cancer Res* 2000;6:1093–1103.

Rajagopalan H, Bardelli A, Lengauer C, Kinzler KW, Vogelstein B, Velculescu VE: Tumorigenesis: RAF/RAS oncogenes and mismatch repair status. *Nature (London)* 2002;418:934.

Reed S. I., Bailly E., Dulic V., Hengst L., Resnitzky D., Slingerland J. G1 control in mammalian cells. *J. Cell Sci.*, 18 (*Suppl.*): 69-73, 1994.

Rodriguez J M, Parrilla P, Moreno A, Sola J, Pinero A, Ortiz S, Soria T: Insular carcinoma: an infrequent subtype of thyroid cancer. *J. Am. Coll. Surg* 1998;187, 503–508.

Santoro M, Chiappetta G, Cerrato A, Salvatore D, Zhang L, Manzo G, Picone A, Portella G, Santelli G, Vecchio G, Fusco A: Development of thyroid papillary carcinomas secondary to tissue specific expression of the RET/PTC1 oncogene in transgene mice. *Oncogene* 1996;12:1821–1826.

Schwaller J, Anastasiadou E, Cain D, Kutok J, Wojiski S, Williams IR, LaStarza R, Crescenzi B, Sternberg DW, Andreasson P, Schiavo R, Siena S, Mecucci C, Gilliland DG: H4(D10S170), a gene frequently rearranged in papillary thyroid carcinoma, is fused to the platelet-derived growth factor receptor beta gene in atypical chronic myeloid leukemia with t(5;10)(q33;q22). *Blood*. 2001 Jun 15;97(12):3910-8

Sherr C. J., Roberts J. M: Inhibitors of mammalian G1 cyclin-dependent kinases. *Genes Dev.*, 10: 1149-1163, 1995.

Shiloh Y: ATM: ready, set, go. *Cell Cycle*. 2003 Mar-Apr;2(2):116-7.

Soares P, Trovisco V, Rocha AS, Lima J, Castro P, Preto A, Máximo V, Botelho T, Seruca R, Sobrinho-Simões M: BRAF mutations and Ret/PTC rearrangements are alternative events in the etiopathogeneses of PTC. *Oncogene* 2003;32:4578–4580.

Soares P, Trovisco V, Rocha AS, Lima J, Castro P, Preto A, Máximo V, Botelho T, Seruca R, Sobrinho-Simões M: BRAF mutations typical of papillary thyroid carcinoma are more frequently detected in undifferentiated than in insular and insular-like poorly differentiated carcinomas. *Virchows Arch* 2004;444:572–576.

Sobrinho-Simoes M, Preto A, Rocha AS, Castro P, Máximo V, Fonseca E, Soares P: Molecular pathology of well differentiated thyroid carcinomas. *Virchows Arch* 2005;447:787–793.

Suarez HG, Du Villard JA, Severino M, Caillou B, Schlumberger M, Tubiana M, Parmentier C, and Monier R. Presence of mutations in all three ras genes in human thyroid tumors. *Oncogene* 1990;5:565–70.

Takahashi M, Ritz J, Cooper GM: Activation of a novel human transforming gene, ret, by DNA rearrangement. *Cells* 1985;42: 581–588.

Tallini G, Asa S: RET oncogene activation in papillary thyroid carcinoma. *Adv Anat Pathol* 2001;8:345–354.

Tenbrock K, Juang YT, Leukert N, Roth J, Tsokos GC. The transcriptional repressor cAMP response element modulator alpha interacts with histone deacetylase 1 to repress promoter activity. *J Immunol*. 2006 Nov

1;177(9):6159-64.

Tong Q, Xing S, Jhian SM: Leucine zipper-mediated dimerization is essential for the PTC1 oncogenic activity. *J Biol Chem*. 1997 Apr 4;272(14):9043-7.

Trovisco V, Vieira de Castro IV, Soares P, Máximo V, Silva P, Magalhães J, Abrosimov A, Guiu XM, Sobrinho-Simões M: BRAF mutations are associated with some histological types of papillary thyroid carcinoma. *J Pathol* 2004;202:247–251.

Trovisco V, Soares P, Preto A, de Castro IV, Lima J, Castro P, Máximo V, Botelho T, Moreira S, Meireles AM, Magalhães J, Abrosimov A, Cameselle-Teijeiro J, Sobrinho-Simões M: Type and prevalence of BRAF mutations are closely associated with papillary carcinoma histotype and patients' age but not with tumor aggressiveness. *Virchows Arch* 2005;446:589–595.

Trovisco V, Soares P, Sobrinho-Simoes M: B-RAF mutations in the etiopathogenesis, diagnosis and prognosis of thyroid carcinomas. *Hum Pathol* 2006;37:781–786.

van der Laan BF, Freeman JL, Tsang RW. & Asa SL. The association of well-differentiated thyroid carcinoma with insular or anaplastic thyroid carcinoma: evidence for dedifferentiation in tumor progression. *Endocr. Pathol* 1993;4, 215–221.

Viglietto G, Chiappetta G, Martinez-Tello FJ, Fukunaga FH, Tallini G, Rigopoulou D, Visconti R, Mastro A, Santoro M, Fusco A. RET/PTC oncogene activation is an early event in thyroid carcinogenesis. *Oncogene*. 1995 Sep 21;11(6):1207-10.

World Health Organization Classification of Tumours. Pathology and Genetics of Tumours of Endocrine Organs eds DeLellis R. A., Lloyd R. V., Heitz, P. U. & Eng, C 2004 IARC Press, Lyon,

Xing M, Westra WH, Tufano RP, Cohen Y, Rosenbaum E, Rhoden KI, Carson KA, Vasko V, Larin A, Tallini G, Tolaney S, Holt EH, Hui P, Umbricht CB, Basaria S, Ewertz M, Tufaro AP, Califano JA, Ringel MD, Zeiger MA, Sidransky D, Ladenson PW: BRAF mutation predicts a poorer clinical prognosis for papillary thyroid cancer. *J Clin Endocrinol Metab* 2005;90:6373–6379.

Xing M. BRAF mutation in thyroid cancer. *Endocr Relat Cancer* 2005;12:245–62.

Xu X, Quiros RM, Gattuso P, Ain KB, Prinz RA: High prevalence of BRAF

gene mutation in papillary thyroid carcinoma and thyroid tumor cell lines.
Cancer Res 2003;63:4561–4567.